

Two-stage Distributionally Robust Optimization for Cross-dock Door Design

Laureano F. Escudero¹. laureano.escudero@urjc.es

M. Araceli Garín². mariaaraceli.garin@ehu.eus

Aitziber Unzueta³. aitziber.unzueta@ehu.eus

1. Area of Statistics and Operations Research, Universidad ReyJuan Carlos, URJC, Móstoles (Madrid), Spain.
2. Quantitative Methods department, Universidad del País Vasco, UPV/EHU, Bilbao (Bizkaia), Spain.
3. Applied Mathematics department, Universidad del País Vasco, UPV/EHU, Bilbao (Bizkaia), Spain.

ABSTRACT

The cross-dock door design problem consists of deciding the strip and stack doors and nominal capacity of an entity under uncertainty. Inbound commodity flow from origin nodes is assigned to the strip doors, it is consolidated in the entity, and the outbound flow is assigned to the stack ones for being delivered to destination nodes, at a minimum cost. The problem combines three highly computational difficulties, namely, NP-hard combinatorics, uncertainty in the main parameters and their probability distribution. Distributionally robust optimization is considered to deal with these uncertainties. Its related two-stage mixed binary quadratic model is presented for cross-dock problem-solving; the first stage decisions are related to the design of the entity; the second stage ones are related to the assignment of the commodity flow to the doors in a finite set of scenarios for the ambiguity set members. The goal is to minimize the highest total cost in the ambiguity set, subject to the constraint system for each of those members and the stochastic dominance risk averse functional. As far as we know, the challenging problem that results has not been addressed before, although its application field is a very broad one. Given the problem-solving difficulty, a scenario cluster decomposition and a *min-max* based matheuristic are proposed for obtaining lower and upper bounds, respectively. A computational study validates the proposal; it overperforms the straightforward use of the state-of-the-art solvers Cplex and Gurobi.

KEYWORDS

Combinatorial Optimization; cross-dock door design; two-stage distributionally robust; stochastic dominance; bounds.

1 Introduction and motivation

As it is known, given a network with commodities to deliver from origin nodes to destination ones, the cross-docking problem basically consists of using an entity to serve as a consolidation point for helping on supply chain distribution. The origin nodes can deliver the commodities in the cross-dock (CD) entity, through so-named strip doors, so that after being classified by type and destination they can be transported (usually, in smaller quantities) to the destination nodes, through so-named stack doors. A panoramic of a real CD entity is shown in Fig. 1 and the classical operation process of the entity is depicted in Fig. 2, taken from [Escudero et al. \(2024a\)](#).

One of the optimization problems in cross-docking is the deterministic so-named Cross-dock Door



Figure 1: CD entity - Guadalajara (Spain). Source:Alimarket

Assignment Problem (CDAP). In this case, the set of strip and stack available doors is given as well as the related capacity. Additionally, the set of origin and destination nodes is also known jointly with the commodity volume to serve. Even considering those sets and parameters as deterministic ones, CDAP is a difficult binary quadratic combinatorial problem. Its constraint system is composed of two Generalized Assignment Problems (GAP), one is related to the strip doors and the other problem is related to the stack ones, where the origin nodes and the destination ones are to be assigned, respectively. Those two problems are linked by quadratic terms in the objective function, see [Escudero et al. \(2024a\)](#). For good overviews on cross-docking applications, see [Akkerman et al. \(2022\)](#), [Kiani Mavi et al. \(2020\)](#), [Serrano et al. \(2021\)](#), among others.

The treatment of the cross-docking problem-solving is a young discipline from an academic view; as a matter of fact, most of the literature has been published during the last 25 years. See different approaches for CDAP solving and comprehensive reviews in [Goodarzi et al. \(2020\)](#), [VanBelle et al. \(2012\)](#), mainly for metaheuristic algorithms. In particular, see [Escudero et al. \(2024a\)](#), [Gelareh et al. \(2020\)](#), [Goodarzi et al. \(2020\)](#), [Guignard \(2020\)](#), [Guignard et al. \(2012\)](#), [Nassief et al. \(2019\)](#), among others.

As an extension of CD usage, [Asgharyar et al. \(2025\)](#) present a mixed integer linear programming (MILP) model for an integration framework of the vehicle routing problem and the CD assignment and scheduling one with no uncertainty in the parameters. The vehicles are assigned to origin nodes (i.e., suppliers) and destination ones (i.e., retailers) at each period (a day) along a time horizon (a week), where the vehicle capacity is considered but not the capacity of the CD entity for commodity handling. The goal consists of optimizing vehicle scheduling and routing, and loading and unloading commodity volumes in the CD entity at each period, so that the retailers' demand is satisfied along the time horizon at the minimum cost. A matheuristic algorithm is introduced for problem-solving based on several variants of the variable neighborhood search methodology. A comprehensive literature overview on vehicle routing and CD usage is also provided.

Comprehensive reviews on CDAP under uncertainty are also recently published in [Ardakani and Fei \(2020\)](#), [Buakum and Wisittipanich \(2019\)](#). [Goodarzi et al. \(2020\)](#) presents an approach for disruption

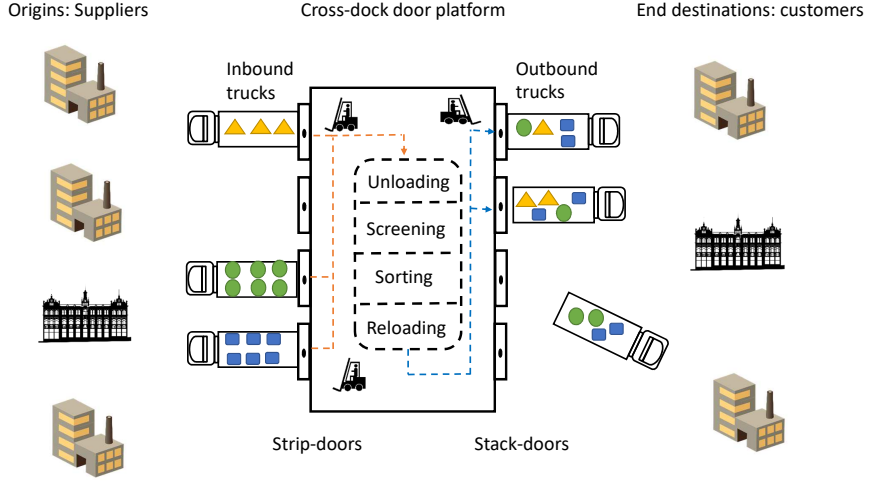


Figure 2: CD entity

issues in the truck scheduling problem; it proposes a column and constraint generation exact algorithm for problem-solving. (See a review in [Boysen and Fliedner \(2010\)](#) for the deterministic version of the problem). See also [Xi et al \(2020\)](#) for uncertainty on arrival and operational times. [Altaf et al. \(2025\)](#) present an approach for solving CDAP by considering truck dock assignment with temporary storage under uncertainty in truck arrival times. A robust approach and a polyhedral representation of the uncertainty are considered plus a Montecarlo scheme for simulating the realizations. [Chargui et al. \(2021\)](#) introduce a Physical Internet (PI)-based truck scheduling problem, where a CD entity to transfer products from origin nodes to destinations ones is considered, and the uncertainty lies in the trucks' arrival times. A multi-objective MILP model is presented to minimize the number of trucks, PI-containers and total tardiness. A fuzzy chance-constrained-based approach is considered for problem-solving.

Another important problem in cross-docking is the so-named Cross-dock Door Design Problem (CDDP), the subject of this work. Here, the set of strip and stack available doors is not given, not its capacities and, on the other hand, the sets of origin and destination nodes are uncertain jointly with the inbound and outbound commodity volume to serve. Moreover, the literature on CDDP is very scarce. Basically, the CD door design is considered within a supply network design planning along a time horizon under uncertainty, where details of each individual door are usually not taken into account. Two works that are representative of the state-of-the art on the issue are [Mousavi et al. \(2014\)](#) and [Soanpet \(2012\)](#). In particular, the first work considers locations of multiple CD centers and vehicle routing scheduling along a time horizon. An hybrid of fuzzy possibilistic and stochastic MILP optimization approaches is introduced to cope with uncertain parameters. Two stochastic models are presented in [Soanpet \(2012\)](#)

for CDDP where the problem consists of a multi-commodity supply network design for given sets of origin and destination nodes. The individual doors and their capacities are not considered for the CD centers, nor the commodity assignment. The first model is a chance constraint stochastic integer quadratic one to locate a given number of centers. The uncertainty lies in their capacity by assuming to follow the Normal Distribution. The second model is a two-stage stochastic mixed binary quadratic (MBQ) one, where the uncertainty lies in the centers' capacity disruption. Binary linear optimization models are presented in [Essghaier et al. \(2021\)](#) and [Miao et al. \(2014\)](#) for assignment trucks to doors in a given CD entity that simultaneously minimizes the handling and transportation cost within a time window. No commodity volume bounds are considered in any door. The former deals with the problem expansion in two flavours, first, allowing a collaboration of supply competitors, such that the doors of one of them can be used by any other at a given rental cost. And, second, the commodity handling and transportation time is an uncertain parameter to be modeled as a triangular fuzzy number, so that a fuzzy chance-constrained-based approach is considered for problem-solving. [Miao et al. \(2014\)](#) deals with the deterministic version of the problem, and a tabu-search algorithm is presented for problem-solving. A genetic metaheuristic algorithm is presented in [Gallo et al. \(2022\)](#) for solving a two-stage stochastic MILP model in a CD entity. The goal is to minimize the earliness and tardiness penalty costs of commodity delivering. An efficient heuristic, so-named Stability Approach, is presented in [Fonseca et al. \(2024\)](#) for solving multi-dock truck scheduling problems, where the uncertainty lies in the truck release dates. [Taheri and Taft \(2024\)](#) present a multi-objective robust MILP approach for scheduling and routing vehicles through a multi CD system, taking into account uncertain demand. A location selection of CD entities in urban areas is dealt with in [Wang et al. \(2024\)](#). An approach is introduced based on data development analysis and multi-attribute border approximation schemes, among other ones, for dealing with strategic, tactical and operational decisions.

An important piece of information to deal with in practical applications as CDDP is the probability distribution (PD) followed by the uncertainty in the main parameters. It is usually unknown, being the motivation for Distributionally Robust Optimization (DRO), where a set of PDs is dealt with as a counterpart of the truly underlying PD. Knight associated in 1921 *risk* with the randomness of a realization from known PD and uncertainty (in today terminology, *ambiguity*) with the situation where the true PD is unknown, see [Knight \(2012\)](#) and also [Caunhye and Alem \(2023\)](#). To the best of our knowledge, [Scarf \(1957\)](#) is the first to consider DRO (although without using the name), for solving the problem: Purchasing a quantity of an item for reselling it in advance to knowing the demand (i.e., the news vendor problem), where the mean and variance are assumed to be known. The goal consists of maximizing the minimum profit for demands following PDs that share those two moments. So, a modeler-driven PD set can be considered for generating an ambiguity set.

There is a broad literature where a given bound for the distance of a PD set to a Nominal Distribution (ND) is considered. The variety of measures to define that distance include the popular Wasserstein distance introduced in [Kantorovich \(1942\)](#), also known as the translation of masses or Earth mover model;

the ϕ divergences as versions of the χ^2 distance, the Kullback-Leibler divergence, the Hellinger distance, and the Burg entropy (see Bayraksan et al. (2024), Philpott et al. (2018), among others); the nested distance (Pflug and Pichler (2014)); the ℓ_1 and ℓ_∞ norms defining distances (Xie (2020), Wang et al. (2023)); the ∞ -Wasserstein distance (Bertsimas et al. (2022)); and others. A new family of ϕ divergence functions is introduced in Caunhye and Alem (2023), it is based on infima convolution, piecewise linearity and the Moreau-Yosida regularization. DRO considering stochastic dominance was introduced in Dentcheva and Ruszczyński (2010), establishing its optimality conditions, see also Dentcheva and Ruszczyński (2014). Some second-order stochastic dominance continuous DRO approaches have been presented in Mei et al. (2022), among others, where the Wasserstein metric defines the ambiguity set in the neighbourhood ball centered in a ND. Recently, a work on DRO for potassium fertilizer product transportation is presented in Jiang et al. (2024), where the inventory level and transshipment is performed in a CD network under uncertainty along a given time horizon. The original DRO model is transformed in a second-order cone optimization one based on duality theory.

CDDP-DRO description as a subject of this work

CDDP consists of deciding on the doors' selection and their nominal capacity under uncertainty in a given CD entity. The problem combines three highly computational difficulties, namely, NP-hard quadratic combinatorics, uncertainty in the main parameter sets and the parameters themselves, and ambiguity in the truly PD that is followed by the sets and parameters. The uncertainty mainly lies in the sets of origin and destination nodes and, then, in the commodity volume from origins to destinations. The other sources of uncertainty lie in the handling and transportation cost through the CD entity and the door capacity disruption. There are two types of node-door assignments: the standard procedure and the outsourcing one. The latter must be considered when either no strip door is available for an inbound commodity flow, or no stack door is available for exiting an outbound commodity flow. Outsourcing means are required in both cases.

Notice that CDDP could be represented by a two-stage stochastic MBQ model, where the first stage decisions are related to the design of the CD entity and the second stage ones are related to the assignment of inbound and outbound commodity flows to the strip and stack doors. The assignment in that option is performed under a unique finite set of scenarios, which represent the realizations of the uncertain parameters, see Escudero et al. (2024b). The approach is very attractive when the set of scenarios is relatively close to the truly underlying PD followed by the uncertain parameter sets and the parameters themselves. Moreover, the alternative that is proposed in this work considers the case where the truly PD is not known; it adds an additional difficulty to deal with. The scheme considers a two-stage DRO for getting better accuracy on dealing with the uncertainty, since it is represented by an ambiguity set, where each member is composed of a set of scenarios. Toward this end, it is assumed that a so-named ND is available, as composed of a scenario set to represent the realization of the uncertain parameters. So, the CDDP problem-solving may require a DRO scheme composed of the three following ingredients: first, a

scheme for the ambiguity set generation; second, a distributionally robust deterministic equivalent MBQ modeling paradigm to consider the ambiguity set; and, third, a decomposition matheuristic methodology, since its solving up to optimality could be unaffordable in reasonable computing effort, given the difficulty of the intrinsic CDDP-DRO problem-solving and the huge model's dimensions,

1.1 Main contributions and work organization

Combining all above elements results in a new challenging problem that, as far as we know, it has not been addressed before, although its application field is a very broad one. The main contributions of the work are as follows:

1. A scheme is proposed for generating an ambiguity set for the uncertain parameters and related sets, see Section 2. The set is generated from the projection of appropriate perturbations on the cumulative distribution functions (*cdf*) of the ND second stage realizations in a modeler-driven PD set. Those projections should satisfy a given radius in the Wasserstein distance with respect to ND; as a matter of fact, any ϕ -divergence measure could also be used, see Pardo (2005). The underline assumption is that the realizations of the uncertain parameters are independent random variables and those that belong to the same group are identically distributed. On the other hand, the approach considers that the uncertain parameters may belong to non-necessarily disjoint scenario groups. It is worth to point out that the uncertainty lies not only in the parameters' realization but also in the same parameter set. So, a scenario set is generated for each ambiguity set member.
2. A two-stage DRO MBQ model is proposed to explicitly dealing with the ambiguity set in the objective function as well as the constraint system. The goal consists of minimizing the highest cost in the ambiguity set members. The cost for each member is included by the one related to the CD building (first stage decisions) plus the expected cost of the node-to-door assignment in its scenarios (second stage decisions). Given the special structure of the problem and the high dimensions of realistic instances, a mathematically equivalent model so-named Linearized mixed Integer Programming Problem (LIP) is introduced. The cost function minimization is subject to the constraint system for each ambiguity set member. See Section 3 for the Risk Neutral (RN) version.
3. A high negative impact in the cost objective function should be prevented for those scenarios that have also a low probability (i.e., the so-named black swan scenarios). For that purpose, a second-order Stochastic Dominance (SD) risk averse functional, see Escudero and Monge (2018), is considered for the ambiguity set member that is the robust cost provider in the special CD structure. For that purpose a MBQ scheme is considered. See Section 4.
4. Notice that the model's dimensions can be huge ones, due to the size of the CD entity in realistic instances as well as the cardinality of the scenario set and the one of the ambiguity set itself. A

sophisticated scenario cluster decomposition (SCD) is introduced for obtaining a set of candidate first stage solutions as well as a (hopefully, tight) lower bound of the optimal CDDP-DRO solution. It is worth to point out that the combination of DRO and RN, see Section 3.2 and DRO and SD, see Section 4.1, takes benefit of the special structure of the DRO requirements and the CDDP one.

5. A *min-max*-based matheuristic approach is proposed for selecting the first stage solution in the SCD candidate set, and obtaining the related second stage solution of the incumbent CDDP-DRO one; it exploits the special structure of the problem. See Sections 3.4 for RN and 4.3 for SD.

A computational experiment is reported in Section 5 to validate the proposed approach for solving CDDP-DRO; it overperforms the straightforward use of the state-of-the-art solvers Cplex and Gurobi. Section 6 withdraws some conclusions and outlines a future research agenda.

2 On generating the ambiguity set for the second stage uncertain parameters

Let \mathcal{H} denote the set of the uncertain parameters.

The section is organized as follows: Subsection 2.1 presents the assumptions and purpose. Subsection 2.2 introduces a scheme for generating a candidate ambiguity set. Subsection 2.3 deals with generating the ambiguity set, say \mathcal{P} , by considering the Wasserstein distance.

2.1 Assumptions and purpose

- Assumption 1: There is not available enough information on the PD of the uncertainty. Moreover, there is empirical information related to the parameters in set \mathcal{H} . Let the following notation:

Ω , set of scenarios for the uncertain parameters in the so-named ND.

$\hat{\xi}_h^\omega$, realization of uncertain parameter h , for $h \in \mathcal{H}$.

$\hat{\xi}^\omega$, vector of realizations $\{\hat{\xi}_h^\omega \forall h \in \mathcal{H}\}$.

\hat{w}^ω , nominal weight of scenario ω , for $\omega \in \Omega$, so that $\sum_{\omega \in \Omega} \hat{w}^\omega = 1$ and $\hat{w}^\omega > 0$.

The moments are $\hat{\mu}_h = \sum_{\omega \in \Omega} \hat{w}^\omega \hat{\xi}_h^\omega$ and $\hat{\sigma}_h^2 = \sum_{\omega \in \Omega} \hat{w}^\omega (\hat{\xi}_h^\omega - \hat{\mu}_h)^2$, for $h \in \mathcal{H}$.

- Assumption 2: A set of PD types, say \mathcal{Q} , is available for the uncertain parameters. It is also assumed that the parameters are independent random variables, such that those that belong to a group share the same PD. Let the following notation:

\mathcal{G} , set of groups of the uncertain parameters.

$\mathcal{H}_g \subseteq \mathcal{H}$, parameter set that belong to group g and, then, $g(h)$ is the group which parameter h belongs to, for $g \in \mathcal{G}$, such that $\mathcal{H} = \bigcup_{g \in \mathcal{G}} \mathcal{H}_g$.

$\mathcal{Q}_g \subseteq \mathcal{Q}$, PD set that can be followed by the parameters in group g , for $g \in \mathcal{G}$, such that $\mathcal{Q} = \bigcup_{g \in \mathcal{G}} \mathcal{Q}_g$.

$q(g)$, PD independently followed by the parameters in group g , for $q(g) \in \mathcal{Q}_g$, $g \in \mathcal{G}$.

$q(g(h))$, PD followed by parameter h , where $q(g(h)) = q(g(h'))$, for $h, h' \in \mathcal{H}_g$, $g \in \mathcal{G}$ (i.e., the parameters that belong to the same group, share the same PD).

- Assumption 3: The set of the parameters could be uncertain itself. It is the case of the sets of the origin and destination nodes in CDDP, see Section 3.1. Let the following notation:

\mathcal{L} , set of scenario groups, where the realization of some parameters is performed.

$\mathcal{H}^\ell \subseteq \mathcal{H}$, set of parameters that belong to scenario group ℓ , for $\ell \in \mathcal{L}$. Note: $\mathcal{H}^\ell \cap \mathcal{H}^{\ell'} \neq \emptyset$ is allowed for $\ell, \ell' \in \mathcal{L} : \ell \neq \ell'$. It is the case where some parameters do belong to more than one group (as the disruption fraction of the doors' capacity), see Section 3.1. Also $\mathcal{H} = \bigcup_{\ell \in \mathcal{L}} \mathcal{H}^\ell$.

$\Omega^\ell \subseteq \Omega$, set of scenarios in group ℓ , for $\ell \in \mathcal{L}$. Also $\Omega = \bigcup_{\ell \in \mathcal{L}} \Omega^\ell$.

$\Omega_p \subseteq \Omega$, set of scenarios to be generated for member p in candidate ambiguity set, say, \mathcal{P}'_q , $q \in \mathcal{Q}$, see below.

$\ell(\omega')$, group which scenario ω' belongs to, for $\omega' \in \Omega$.

\tilde{w}^ℓ , weight associated with scenario group ℓ in ND to be expressed as $\sum_{\omega \in \Omega^\ell} \hat{w}^\omega$, for $\ell \in \mathcal{L}$.

The process for generating the ambiguity set roughly has the two following steps:

1. Generate the realization of the uncertain parameters and weights, say vector ξ^ω and w^ω , respectively, for $\omega \in \Omega^\ell \cap \Omega_p$, which index p refers to a member of the candidate ambiguity set, say, \mathcal{P}'_q , for $q \in \mathcal{Q}$, such that the cardinality $|\mathcal{P}'_q|$ is modeler-driven. For that purpose, *appropriate perturbations* are performed on the cumulative distribution function *cdf* of the realizations vector $\hat{\xi}^{\omega'}$ in ND, for $\omega' \in \Omega$, once projected in PD set \mathcal{Q} .
2. Select the ambiguity set \mathcal{P} as a subset of the candidate one $\bigcup_{q \in \mathcal{Q}} \mathcal{P}'_q$, where member p points out to the realization of the uncertain parameters and weights in the related scenarios. For that purpose, the time-honored Wasserstein distance, see Kantorovich (1942), is considered in this work.

2.2 Building the candidate ambiguity set \mathcal{P}'_q , for PD $q \in \mathcal{Q}_g$, $g \in \mathcal{G}$. Proposed scheme

To start with, assign $\Omega_p := \Omega$, for $p \in \mathcal{P}'_q$.

By projecting ND $\hat{\xi}_h^\omega$ in PD q and noting that $q \equiv q(g(h))$, the *cdf* of ND uncertain parameter h can be expressed $\hat{u}_{q,h}^\omega = F_q(\hat{\xi}_h^\omega; \hat{\mu}_h, \hat{\sigma}_h^2) \forall \omega \in \Omega^\ell$ (i.e., the estimated probability of success of variable vector $\xi \in (-\infty, \hat{\xi}_h^\omega)$), for $h \in \mathcal{H}^{\ell(\omega)} \cap \mathcal{H}_g$, $\ell \in \mathcal{L}$, where the probability density function is denoted as $f_q(\hat{\xi}_h^\omega; \hat{\mu}_h, \hat{\sigma}_h^2)$.

The next step consists of generating the ϵ -perturbations, say, $\epsilon_p^\omega \sim N(0, \sigma_\epsilon^2)$. So, the element, say, u_h^ω of the *cdf* subject of our work, for $\omega \in \Omega_p$, $p \in \mathcal{P}'_q$, for PD $q \in \mathcal{Q}_g$, $g \in \mathcal{G}$, is computed as $u_h^\omega = \hat{u}_{q,h}^\omega + \epsilon_p^\omega$, such that it is reset to zero (and, then, $\Omega_p := \Omega_p \setminus \{\omega\}$) for a non-positive value and reset it to 1 for a value greater than 1. Thus, let us define ξ_h^ω as the inverse probability function and, then, $\xi_h^\omega = F_q^{-1}(u_h^\omega; \hat{\mu}_h, \hat{\sigma}_h^2)$, for $\omega \in \Omega_p$, $p \in \mathcal{P}'_q$.

Given the independency assumption of the random variables in vector $\xi^\omega = (\xi_h^\omega \forall h \in \mathcal{H}^{\ell(\omega)} \cap \mathcal{H}_g)$, for $\omega \in \Omega^\ell \cap \Omega_p$, $\ell \in \mathcal{L}$, $p \in \mathcal{P}'_q$, $q \in \mathcal{Q}_g$, $g \in \mathcal{G}$, the likelihood, say L^ω , associated with scenario ω in perturbation p and the related normalized weight w^ω can be expressed

$$L^\omega = \prod_{h \in \mathcal{H}^{\ell(\omega)}} f_{q(p)}(\xi_h^\omega; \hat{\mu}_h, \hat{\sigma}_h^2), \text{ where } q(p) \leftrightarrow p \in \mathcal{P}'_q$$

$$w^\omega = \tilde{w}^{\ell(\omega)} \frac{L^\omega}{\sum_{\omega' \in \Omega^{\ell(\omega)} \cap \Omega_p} L^{\omega'}}, \quad (1)$$

Notice that $q \equiv q(g(h))$. It is easy to show that $\sum_{\omega \in \Omega_p} w^\omega = 1$.

2.3 Wasserstein distance for ambiguity set \mathcal{P} generation

The aim is to generate the ambiguity set \mathcal{P} , so that the realization of the uncertain parameters is represented in a more accurate way. For that purpose, let us select a subset of perturbations $\{p\}$ in set $\bigcup_{q \in \mathcal{Q}} \mathcal{P}'_q$, so that the weighted distance, so-named *proximity* l_p^ρ , is small enough between $(\xi^\omega, w^\omega \forall \omega \in \Omega_p)$ in perturbation p and $(\hat{\xi}^{\omega'}, \hat{w}^{\omega'} \forall \omega' \in \Omega)$ in ND.

There is a broad literature on considering the Wasserstein distance in DRO, see [Beesten et al. \(2024\)](#), [Duque et al. \(2022\)](#), [El Tonbari et al. \(2024\)](#), [Erdogan and Iyenhar \(2006\)](#), [Esfahani and Kuhn \(2015\)](#), [Gao and Kleywegt \(2022\)](#), [Ho-Nguyen and Wright \(2023\)](#), [Hosseini-Nodeh et al. \(2012\)](#), [Shen and Jiang \(2023\)](#), to name a few.

The scheme for generating the ambiguity set \mathcal{P} in the context of this work is as follows:

- Minimize the proximity l_p^ρ of the parameters' realizations.

$$l_p^\rho = \min_{\eta^{\omega, \omega'} \geq 0} \sum_{\omega \in \Omega_p} \sum_{\omega' \in \Omega} d^\rho(\xi^\omega, \hat{\xi}^{\omega'}) \eta^{\omega, \omega'}$$

$$\text{s.to } \sum_{\omega' \in \Omega} \eta^{\omega, \omega'} = w^\omega \quad \forall \omega \in \Omega_p$$

$$\sum_{\omega \in \Omega_p} \eta^{\omega, \omega'} = \hat{w}^{\omega'} \quad \forall \omega' \in \Omega, \quad (2)$$

where $\eta^{\omega, \omega'}$ is the 'transportation' variable from scenario ω to scenario ω' and $d^\rho(\xi^\omega, \hat{\xi}^{\omega'})$ is the distance between perturbation p and ND, computed as $\sum_{h \in \mathcal{H}^{\ell(\omega)} \cap \mathcal{H}^{\ell(\omega')}} (\xi_h^\omega - \hat{\xi}_h^{\omega'})^\rho$, for $\rho = \{1, 2, \infty\}$. Recall: $\Omega_p \subseteq \Omega$.

- Set \mathcal{P} is the subset of candidate members $\{p\}$, such that $l_p^\rho \leq \theta$ up to \bar{p} , where the maximum number \bar{p} and the *radius* θ are modeler-driven parameters.

Note: For easing the presentation, Sections 3 and 4 consider that there is only $|\mathcal{L}| = 1$ scenario group and only $|\mathcal{G}| = 1$ uncertain parameters' group.

3 Two-stage DRO model LIP-RN and its Scenario Cluster Decomposition (SCD)

The section presents the RN version of the Linearized mixed Integer Programming (LIP) model as well as its SCD. It also introduces a scheme for obtaining lower and upper bounds. The uncertainty to be dealt with is represented in a set of scenarios for each member of the ambiguity set as explicitly generated by the scheme presented in the previous section.

CDDP-DRO is an extension of the two-stage stochastic model CDDP-TS that we have presented elsewhere, see Escudero et al. (2024b). The main difference is that the latter assumes that the finite set of scenarios fairly represents the truly PD of the uncertainty in the parameters. As a matter of fact, both approaches share many elements. So, the aim of the section is to present the elements (i.e., parameters, variables and constraints) that directly are related to the ambiguity set treatment. Moreover, for completeness and easy reading, Appendix A, see the supplementary file, takes from Escudero et al. (2024b) the other elements of the model.

The section is organized as follows: Subsection 3.1 presents the ambiguity set-related elements of the CD entity. Subsection 3.2 presents the LIP formulation of model CDDP-DRO in its RN version, so-named model LIP-RN. Subsection 3.3 deals with SCD of the model. Subsection 3.4 introduces a scheme for obtaining (hopefully, tight) lower and upper bounds.

3.1 Cross-dock entity. Elements

First stage sets:

\mathcal{I} , strip door candidates, without including inbound outsourcing 'door' $i = 0$.

\mathcal{K}_i , nominal capacity level for candidate strip door i , for $i \in \mathcal{I}$.

\mathcal{J} , stack door candidates, without including outbound outsourcing 'door' $j = 0$.

\mathcal{K}_j , nominal capacity level for candidate stack door j , for $j \in \mathcal{J}$.

First stage parameters for $i \in \mathcal{I}$, $j \in \mathcal{J}$:

F_{ki} , cost of installing capacity level k in strip door i , for $k \in \mathcal{K}_i$.

F_{kj} , cost of installing capacity level k in stack door j , for $k \in \mathcal{K}_j$.

\bar{I} and \bar{J} , upper bounds on the number of strip and stack doors, respectively, that are allowed for the CD entity.

Second stage sets for origin and destination nodes for ambiguity set member p , for $p \in \mathcal{P}$

Ω_p , lexicographically ordered scenarios.

\mathcal{M}^ω and \mathcal{N}^ω , origin and destination nodes under scenario ω , respectively, for $\omega \in \Omega_p$.

Second stage parameters for origin node m and destination node n under scenario ω in ambiguity set member p , for $m \in \mathcal{M}^\omega$, $n \in \mathcal{N}^\omega$, $\omega \in \Omega_p$, $p \in \mathcal{P}$

w^ω , weight associated with scenario ω .

D_i^ω and D_j^ω , disruption fraction of the nominal capacities of strip door i and stack one j , say S_{ki} and R_{kj} , respectively, see Appendix A in the supplementary file.

H_{mn}^ω , commodity volume to be consolidated in the CD entity from node m to node n .

Note: $\xi^\omega = (D_i^\omega \forall i \in \mathcal{I}; D_j^\omega \forall j \in \mathcal{J}; H_{mn}^\omega \forall m \in \mathcal{M}^\omega, n \in \mathcal{N}^\omega)$.

First stage binary variables for CD entity design in ambiguity set member p , for $p \in \mathcal{P}$

$\alpha_{ki}(\beta_{kj})$, which value 1 means that capacity level k is installed in strip door i (stack door j) and otherwise, 0, for $k \in \mathcal{K}_i$, $i \in \mathcal{I}$ ($k \in \mathcal{K}_j$, $j \in \mathcal{J}$).

Second stage variables for $m \in \mathcal{M}^\omega$, $n \in \mathcal{N}^\omega$, $\omega \in \Omega_p$, $p \in \mathcal{P}$

$\alpha_0^\omega(\beta_0^\omega)$, binary variable which value 1 means that inbound (outbound) "outsourcing door" $i = 0$ ($j = 0$) is considered; otherwise, 0.

v_{minj}^ω , continuous variable that can only take 0-1 values in the context of the model, see [Escudero et al. \(2024b\)](#), such that 1 means that origin node m and destination node n are assigned to strip door i and stack door j , respectively, and otherwise, 0.

3.2 Model LIP-RN

It requires the following additional notation, for $p \in \mathcal{P}$:

C_1 , (first stage) CD building costs for ambiguity set member p , as expressed in (4c).

F^ω , continuous variable that takes the (second stage) CD node-door standard and outsourcing assignment cost under scenario ω , as expressed in (4d), for $\omega \in \Omega_p$.

F_0 , high enough penalization for considering outsourcing 'doors' $i = 0$ and $j = 0$.

u , continuous variable that takes the robust (i.e., highest) cost composed of C_1 plus the expected node-door assignment cost under the scenarios in ambiguity set \mathcal{P}

The deterministic equivalent model LIP-RN of the stochastic one can be expressed

$$z_{RN}^* = \min u \quad (3a)$$

$$\text{s.to } C_1 + \sum_{\omega \in \Omega_p} w^\omega F^\omega \leq u \quad \forall p \in \mathcal{P} \quad (3b)$$

$$\text{cons system (4)}. \quad (3c)$$

Another type of DRO objective function, as an alternative to (3a)-(3b), can be expressed

$$z_{RN}^* = \min \{C_1 + \max_{p \in \mathcal{P}} \{ \sum_{\omega \in \Omega_p} w^\omega F^\omega \} \},$$

where the first stage cost is not considered in the highest expected one, among the ambiguity set members, see Beesten et al. (2024). Moreover, we argue that the CD building cost (i.e., first stage one) is better protected by including it in the robustness provided by constraint (3b). It is obviously assumed that the CD entity is built in both DRO approaches before the parameters' uncertainty is unveiled and, then, it does not depend upon any single ambiguity set member.

$$\alpha_{ki} \in \{0, 1\} \quad \forall k \in \mathcal{K}_i, \quad \sum_{k \in \mathcal{K}_i} \alpha_{ki} \leq 1 \quad \forall i \in \mathcal{I}, \quad \sum_{i \in \mathcal{I}} \sum_{k \in \mathcal{K}_i} \alpha_{ki} \leq \bar{I} \quad (4a)$$

$$\beta_{kj} \in \{0, 1\} \quad \forall k \in \mathcal{K}_j, \quad \sum_{k \in \mathcal{K}_j} \beta_{kj} \leq 1 \quad \forall j \in \mathcal{J}, \quad \sum_{j \in \mathcal{J}} \sum_{k \in \mathcal{K}_j} \beta_{kj} \leq \bar{J} \quad (4b)$$

$$C_1 = \sum_{i \in \mathcal{I}} \sum_{k \in \mathcal{K}_i} F_{ki} \alpha_{ki} + \sum_{j \in \mathcal{J}} \sum_{k \in \mathcal{K}_j} F_{kj} \beta_{kj} \quad (4c)$$

$$F^\omega = F_0(\alpha_0^\omega + \beta_0^\omega) + F(v_{minj}^\omega) \quad \forall \omega \in \Omega_p, p \in \mathcal{P} \quad (4d)$$

$$\text{cons system (A.1) – (A.5), where } \omega \in \Omega \text{ replaced with } \omega \in \Omega_p, p \in \mathcal{P}, \quad (4e)$$

where function $F(v_{minj}^\omega)$ provides the (second stage) CD node-door assignment standard cost under scenario ω , as expressed in (A.6), for $\omega \in \Omega_p$, see Appendix A.

Notice that, as considered in Appendix A, the first stage constraint system (4a)-(4c) defines the doors' building, nominal capacity installation, and related cost. The second stage one (A.1)-(A.4) defines the CD node-door standard and outsourcing assignment constraining under the scenarios in the TS setting. Constraint system (A.5) allows that variable v_{minj}^ω can replace the binary quadratic expression $x_{mi}^\omega y_{nj}^\omega$ in a mathematically equivalent form.

3.3 SCD of model LIP-RN

Observe that a high computing effort may be required for solving model LIP-RN (3) even for medium-sized instances. There is a myriad of decomposition algorithms for solving general two-stage stochastic MILP models, see e.g., Escudero et al. (2016) for a literature overview.

Moreover, notice that, besides the first stage constraints (4a)-(4c), the members of the ambiguity set \mathcal{P} are only linked in the model by variable u ; the overall scheme for problem-solving proposed in this work takes benefit of this special structure, seemingly amenable for scenario cluster deconpostion (SCD).

So, a scheme is presented for providing lower bounds on the solution value of model LIP-RN. For that purpose, let \mathcal{C}_p and \mathcal{C} denote lexicographically ordered scenario cluster sets, where the former is related to member p in \mathcal{P} and $\mathcal{C} = \bigcup_{p \in \mathcal{P}} \mathcal{C}_p$. On the other hand, Ω^c is the scenario set for cluster c in \mathcal{C}_p , for $p \in \mathcal{P}$, so that $\Omega_p = \bigcup_{c \in \mathcal{C}_p} \Omega^c$. This work considers the scenario clustering scheme presented in [Escudero et al. \(2024b\)](#).

A split-variable reformulation of model LIP-RN (3) may help to problem-solving, since a related SCD approach decomposes the model in smaller submodels. Let $f\mathcal{C}$ and $l\mathcal{C}$ denote the first cluster and the last one in set \mathcal{C} , respectively. The notation for the α - and β -variables related to scenario cluster c has been taken from [Escudero et al. \(2024b\)](#), for $c \in \mathcal{C}$.

$a(c), n(c)$, ancestor and next clusters of c in set \mathcal{C} , respectively. By little abusing of the notation, let $n(l\mathcal{C}) = f\mathcal{C}$ and, then, $a(f\mathcal{C}) = l\mathcal{C}$.

α_{ki}^c , copy of variable α_{ki} , for $k \in \mathcal{K}_i, i \in \mathcal{I}$.

β_{kj}^c , copy of variable β_{kj} , for $k \in \mathcal{K}_j, j \in \mathcal{J}$.

C_1^c , copy of variable C_1 .

\tilde{w}^c , weight associated with cluster c , to be expressed as $\sum_{\omega \in \Omega^c} w^\omega$ and, then, $\sum_{c \in \mathcal{C}_p} \tilde{w}^c = 1$, for $p \in \mathcal{P}$.

\tilde{w}^ω , weight associated with scenario ω that belongs to cluster c , to be expressed as $\frac{w^\omega}{\tilde{w}^c}$ and, then, $\sum_{\omega \in \Omega^c} \tilde{w}^\omega = 1$.

Additionally, let u^c be a copy of variable u , for $c \in \mathcal{C}$.

Following [Escudero et al. \(2016\)](#), the Splitting Variable Constraints (SVC) for Risk Neutral, to be notated as SVC-RN, can be expressed in a circular mode, for $c \in \mathcal{C}$:

$$\alpha_{ki}^c - \alpha_{ki}^{n(c)} \leq 0 \quad \forall k \in \mathcal{K}_i, i \in \mathcal{I} \quad (5a)$$

$$\beta_{kj}^c - \beta_{kj}^{n(c)} \leq 0 \quad \forall k \in \mathcal{K}_j, j \in \mathcal{J} \quad (5b)$$

$$u^c - u^{n(c)} \leq 0. \quad (5c)$$

A mathematically equivalent SVC-RN (5)-based model to LIP-RN (3) can be expressed

$$z_{RN}^* = \min u^{\bar{c}} \quad (6a)$$

$$\text{s.to } C_1^{\bar{c}} + \sum_{c \in \mathcal{C}_p} \sum_{\omega \in \Omega^c} \tilde{w}^\omega F^\omega \leq u^{\bar{c}} \quad \forall p \in \mathcal{P} \quad (6b)$$

$$\text{SVC-RN (5)} \quad (6c)$$

cons system (4), where $\alpha_{ki}, \beta_{kj}, C_1$ replaced with $\alpha_{ki}^c, \beta_{kj}^c, C_1^c \forall c \in \mathcal{C}$, and

$$\bar{c} \text{ is any scenario cluster in } \mathcal{C}. \quad (6d)$$

It is worth to point out that, given (5), it results that the variables $(\cdot)^c$ and $(\cdot)^{c'}$ have the same value for $c, c' \in \mathcal{C}$. Similarly, $u^{\bar{c}}$ has the same value as u (3b). Anyway, the model has not any practical value, unless it is used for designing a decomposition approach.

The relaxation of the SVC-RN constraints (5) results in SCD-RN c -submodels (7), for $c \in \mathcal{C}$, to be expressed

$$z_{SCD-RN}^c = \min u^c \quad (7a)$$

$$\text{s.to } C_1^c + \sum_{\omega \in \Omega^c} \tilde{w}^\omega F^\omega \leq u^c \quad (7b)$$

$$\text{cons system (4), where } \alpha_{ki}, \beta_{kj}, C_1 \text{ replaced with } \alpha_{ki}^c, \beta_{kj}^c, C_1^c. \quad (7c)$$

3.4 On obtaining the lower and upper bounds \underline{z}_{RN} and \bar{z}_{RN} of z_{RN}^* in model LIP-RN (3)

The steps of the scheme for obtaining the lower and upper bounds are as follows:

1. On obtaining the lower bound \underline{z}_{RN} :

- (a) Solve SCD c -submodel (7) and retrieve the related objective function value z_{SCD-RN}^c , for $c \in \mathcal{C}$.
- (b) Solve the LP submodel in the B&C rood node after the MILP preprocessing is performed for solving model (3), and retrieve the related objective function value, say, z_{LP-RN} .
- (c) The *max-max* related bound \underline{z}_{RN} can be expressed

$$\underline{z}_{RN} = \max\{z_{LP-RN}, \max_{p \in \mathcal{P}}\{\sum_{c \in \mathcal{C}_p} \tilde{w}^c z_{SCD-RN}^c\}\}. \quad (8)$$

2. On obtaining the upper bound \bar{z}_{RN} :

- (a) Retrieve vector $(\hat{\alpha}^c, \hat{\beta}^c)$ of the first-stage variables $(\alpha_{ki}^c, \beta_{kj}^c, \forall ki, \forall kj)$ from the solution of c -submodel (7) that has been obtained in Step 1(a), and compute the first stage cost, say, \hat{C}_1^c (4c), for $c \in \mathcal{C}$.
- (b) Solve model LIP-RN (3), where the (α, β) -first stage variables are fixed to the solution vector $(\hat{\alpha}^c, \hat{\beta}^c)$, for $c \in \mathcal{C}$, as retrieved in Step 2(b), so that the second stage cost, say, $\hat{F}^{c, \omega}$ (4d) is computed from its solution, for $\omega \in \Omega_p, p \in \mathcal{P}$.
- (c) The *min-max* related bound \bar{z}_{RN} can be expressed

$$\bar{z}_{RN} = \min_{c \in \mathcal{C}}\{\hat{C}_1^c + \max_{p \in \mathcal{P}}\{\sum_{\omega \in \Omega_p} w^\omega \hat{F}^{c, \omega}\}\}. \quad (9)$$

4 Two-stage DRO model LIP-SD and its SCD

As a counterpart of model LIP-RN (3), the risk averse SD version and its SCD are introduced as well as a scheme for obtaining (hopefully, tight) lower and upper bounds.

4.1 Model LIP-SD

The aim of model LIP-SD consists of preventing, up to some extent, the high cost composed of the (first stage) entity building cost C_1 (4c) and the (second stage) node-to-door assignment cost F^ω (4d) under the so-named black swan scenarios (i.e., ones with low weight and high cost). The reason is that this cost can be balanced in model LIP-RN (3) with the small one in other scenarios, for the selected member p in the ambiguity set \mathcal{P} . Notice that the prevention of that high cost affects the highest expected cost u (3b) and, then, it may affect the door selection, its capacity and the related first stage cost. It can even affect the ambiguity set member that provides cost u .

The literature on DRO risk averse is very scarce and, as far as we know, it is restricted to CVaR, see Ghaoui et al. (2003), Huong et al. (2008), Tong et al. (2009), Zhai et al. (2025), Zhu et al. (2009). Moreover, the SD risk averse measure allows to deeply influence on the prevention of negative implications of black swan scenarios; see some variations in Dentcheva and Ruszczyński (2003, 2014), Escudero et al. (2020), Escudero and Monge (2018, 2023), Gollmer et al. (2011), Hosseini-Nodeh et al. (2012), Pichler (2024), Shapiro (2021), Shapiro et al. (2009), Cesarone and Puerto (2025), Dentcheva and Yi (2025), among others. In our case, the goal is to keep reduced the impact of those scenarios in different levels of the CDDP cost under modeler-driven bounds in given policy profiles.

For that purpose, let γ_p be a binary variable, which value 1 means that ambiguity set \mathcal{P} member p is the provider of the robust cost u and otherwise, 0, for $p \in \mathcal{P}$. Additionally, let \underline{u} and \bar{u} denote the highest possible lower bound and the smallest upper one of variable u that the problem allows it, respectively.

The constraint system can be expressed

$$\underline{u}(1 - \gamma_p) + u \gamma_p \leq C_1 + \sum_{\omega \in \Omega_p} w^\omega F^\omega \leq u \quad \forall p \in \mathcal{P}. \quad (10)$$

Notice the difference between the MBQ term in (10) for SD and the linear one (3b) for RN, where the γ -variables are not required in the latter. Moreover, the expression $u \gamma_p$ in the left-hand-side of (10) can be mathematically equivalent to its replacement with variable u_p plus the appending of the time-honored Fortet linear inequalities (11d), see Fortet (1960), McCormick (1976). From where the MILP u -constraint system can be expressed

$$\underline{u}(1 - \gamma_p) + u_p \leq C_1 + \sum_{\omega \in \Omega_p} w^\omega F^\omega \quad \forall p \in \mathcal{P} \quad (11a)$$

$$C_1 + \sum_{\omega \in \Omega_p} w^\omega F^\omega \leq u \quad \forall p \in \mathcal{P} \quad (11b)$$

$$\sum_{p \in \mathcal{P}} \gamma_p = 1 \quad (11c)$$

$$u_p \leq \bar{u} \gamma_p, u_p \leq u, u \leq u_p + \bar{u}(1 - \gamma_p), \quad \gamma_p \in \{0, 1\} \quad \forall p \in \mathcal{P}. \quad (11d)$$

Observe that the constraint system (11a)-(11b) is satisfied with strict equality for the member p that provides the highest cost, where the Special ordered set S1-based constraint (11c) defines the variable γ_p to be selected.

The notation of the SD elements is as follows:

- $C_{12}^\omega = C_1 + F^\omega$, total cost composed of the first stage one and the second stage cost under scenario ω in ambiguity set member p , for $\omega \in \Omega_p$, $p \in \mathcal{P}$. Let \bar{C} denote its upper bound.
- \mathcal{B} , policy profile set on the total scenario cost in any ambiguity set member p , for $p \in \mathcal{P}$.
- Parameters for profile b , for $b \in \mathcal{B}$:
 - ι^b , cost threshold as a target under any scenario ω , for $\omega \in \Omega_p$, $p \in \mathcal{P}$. An appropriate value could be smaller than cost C_{12}^ω for one scenario, at least, provided that second stage cost F^ω is part of the highest expected one in the definition of u in (11).
 - \bar{s}^b , upper bound on the cost surplus over threshold ι^b under any scenario.
 - $\bar{\bar{s}}^b$, upper bound on the expected cost surplus over threshold ι^b in the scenarios.
- Continuous variable:
 - $s^{\omega,b}$, cost surplus over threshold ι^b under scenario ω , for $\omega \in \Omega_p$, $p \in \mathcal{P}$, $b \in \mathcal{B}$.
- MBQ term:
 - $C_{12}^\omega \gamma_p$, cost under scenario ω in the definition of u (11), provided that $p \in \mathcal{P} : \gamma_p = 1$, and otherwise, 0. Notice that the term can be replaced with the variable $C_{12,p}^\omega$ plus the appending of the related Fortet linear inequalities (12d).

The SD constraint system can be expressed

$$C_{12}^\omega = C_1(4c) + F^\omega(4d) \quad \forall \omega \in \Omega_p, p \in \mathcal{P} \quad (12a)$$

$$C_{12,p}^\omega - s^{\omega,b} \leq \iota^b, \quad 0 \leq s^{\omega,b} \leq \bar{s}^b \quad \forall \omega \in \Omega_p, p \in \mathcal{P}, b \in \mathcal{B} \quad (12b)$$

$$\sum_{\omega \in \Omega_p} w^\omega s^{\omega,b} \leq \bar{\bar{s}}^b \quad \forall p \in \mathcal{P}, b \in \mathcal{B} \quad (12c)$$

$$C_{12,p}^\omega \leq \bar{C} \gamma_p, C_{12,p}^\omega \leq C_{12}^\omega, C_{12}^\omega \leq C_{12,p}^\omega + \bar{C}(1 - \gamma_p) \quad \forall \omega \in \Omega_p, p \in \mathcal{P} \quad (12d)$$

Constraints (12b) define the bounded cost surplus over the threshold for the policy profile under any scenario. Constraints (12c) bound the expected cost surplus in the scenarios. It can be shown that SD is a coherent risk averse measure, as defined in Artzner et al. (1999), since it satisfies the properties translation invariance, positive homogeneity, monotonicity and convexity. Additionally, it is a time consistent risk averse measure, see Escudero and Monge (2018).

So, model LIP-SD can be expressed

$$\begin{aligned} z_{SD}^* &= \min u \\ \text{s.to cons system } (4), (11), (12). \end{aligned} \quad (13)$$

Notice that $u_p = 0$, and $C_{12,p}^\omega = 0$ for $\omega \in \Omega_p, p \in \mathcal{P} : \gamma_p = 0$, see S1 (11c).

4.2 SCD of model LIP-SD

A high computing effort may be required for solving model LIP-SD (13) even for medium-sized instances, being much higher than the effort for solving model LIP-RN (3). Moreover, notice that, besides the first stage constraints (4a)-(4b), the members of the ambiguity set \mathcal{P} are linked in the model with constraint system (11). The overall scheme for problem-solving proposed in this work takes benefit of the model's special structure, seemingly amenable for SCD.

For the decomposition purposes, let γ_p, u_p, u from (11) be replaced with $\gamma^c, u_c, u^c \forall c \in \mathcal{C}_p, p \in \mathcal{P}$.

So, the constraint system SVC-SD can be expressed

$$\text{cons system } SVC - RN(5) \quad \forall c \in \mathcal{C} \quad (14a)$$

$$\gamma^c - \gamma^{n(c)} \leq 0 \quad \forall c \in \mathcal{C}_p, p \in \mathcal{P}. \quad (14b)$$

Let also \tilde{c} denote any scenario cluster in $\mathcal{C}_p, p \in \mathcal{P}$. A mathematically equivalent SVC-SD (14)-based model LIP-SD (13) can be expressed

$$z_{SD}^* = \min u^{\tilde{c}} \quad (15a)$$

$$\text{s.to } \underline{u}(1 - \gamma^c) + u_c \leq C_1^{\tilde{c}} + \sum_{c' \in \mathcal{C}_p} \sum_{\omega \in \Omega^{c'}} \tilde{w}^\omega F^\omega \quad \forall c \in \mathcal{C}_p, p \in \mathcal{P} \quad (15b)$$

$$C_1^{\tilde{c}} + \sum_{c' \in \mathcal{C}_p} \sum_{\omega \in \Omega^{c'}} \tilde{w}^\omega F^\omega \leq u^{\tilde{c}} \quad \forall p \in \mathcal{P} \quad (15c)$$

$$u_c \leq \bar{u}\gamma^c, u_c \leq u^c, u^c \leq u_c + \bar{u}(1 - \gamma^c), \quad \gamma^c \in \{0, 1\} \quad \forall c \in \mathcal{C}_p, p \in \mathcal{P} \quad (15d)$$

(4), (11c), (12), (14), where

γ_p, Ω_p replaced with γ^c, Ω^c for $c \in \mathcal{C}_p, p \in \mathcal{P}$,

α_{ki}, β_{kj} replaced with $\alpha_{ki}^c, \beta_{kj}^c$ for $c \in \mathcal{C}$, and

C_1 replaced with $C_1^{\tilde{c}}$. (15e)

The relaxation of the constraint systems S1 (11c), which implies the one of the γ -requirements, and SVC-SD (14) results in SCD-SD c -submodels (16), for $c \in \mathcal{C}$, to be expressed

$$z_{SCD-SD}^c = \min u^c \quad (16a)$$

$$\text{s.to } \underline{u} \leq C_1^c + \sum_{c' \in \mathcal{C}_p} \sum_{\omega \in \Omega^{c'}} \tilde{w}^\omega F^\omega \leq u^c \quad (16b)$$

cons system (4), (12a), (12b), (12d), where

$$\alpha_{ki}, \beta_{kj}, C_1, \Omega_p \text{ replaced with } \alpha_{ki}^c, \beta_{kj}^c, C_1^c, \Omega^c. \quad (16c)$$

4.3 On obtaining the lower and upper bounds \underline{z}_{SD} and \bar{z}_{SD} of z_{SD}^* in model LIP-SD (13)

The scheme for obtaining the lower and upper bounds follows the same pattern for the RN version, see Section 3.4, so that the *max-max* bound \underline{z}_{SD} can be expressed

$$\underline{z}_{SD} = \max\{z_{LP-SD}, \max_{p \in \mathcal{P}}\{\sum_{c \in \mathcal{C}_p} \tilde{w}^c z_{SCD-SD}^c\}\}, \quad (17)$$

where z_{LP-SD} denotes the LP solution value in the B&C root node after the MILP preprocessing for solving model (13), and z_{SCD-SD}^c is the objective function value retrieved from the solution of SCD c -submodel (16).

On the other hand, the *min-max* related upper bound \bar{z}_{SD} can be expressed

$$\bar{z}_{SD} = \min_{c \in \mathcal{C}}\{\hat{C}_1^c + \max_{p \in \mathcal{P}}\{\sum_{\omega \in \Omega_p} w^\omega \hat{F}^{c,\omega}\}\}, \quad (18)$$

where \hat{C}_1^c is the cost computed as (4c) for vector $(\hat{\alpha}^c, \hat{\beta}^c)$, which is retrieved from the solution of the first stage variables (α, β) in model (16) $\forall c \in \mathcal{C}$, and $\hat{F}^{c,\omega}$ is the second stage cost computed as (4d), which is retrieved from the solution of model (13), where the variables (α, β) are fixed to $(\hat{\alpha}^c, \hat{\beta}^c)$, for $c \in \mathcal{C}_p, p \in \mathcal{P}$.

Note: The proposed scheme cannot even guarantee that the solution of model LIP-SD is feasible for the SD constraint (12c). The potential infeasibility can be expressed, if positive, as $\sum_{\omega \in \Omega_p} w^\omega \hat{s}^{\omega,b} - \bar{s}^b \forall p \in \mathcal{P}, b \in \mathcal{B}$, where $\hat{s}^{\omega,b}$ is the ι^b -related cost surplus in the solution.

It is worthy to remark that there is a high computational complexity in the special structure of models LIP-RN and LIP-SD. Additionally, the structure of the submodels CDAP that are embedded in the second stage constraint system has also a high complexity for each scenario in the ambiguity set members, once the first stage variables are fixed. The decomposition approach considers the constructive matheuristic that we have recently introduced in Escudero et al. (2024b).

Appendix B in the supplementary file presents a Lagrangean Decomposition (LD) of models LIP-RN (3) and LIP-SD (13) as a scheme that dualizes some constraints and Lagrangean relaxes some others. Moreover, the solving of CDDP-DRO is so-complex that any LD decomposition iteration can require high computational effort, see also Escudero et al. (2024a). On the other hand, the weak LD lower bound increasing does not pay the effort. It is mainly due to the inefficient Lagrangean updating scheme to deal with CDDP, even when it is based on the state-of-the-art schemes that are referenced in the appendix.

5 Computational experiment

The section presents the computational experience carried out on some of the instances, say I1, I3 and I7, taken from Escudero et al. (2024b), in order to show the effectiveness of the proposed approach. In particular, the instances have 5, 10 and 20 scenarios each one as data in ND from where the ambiguity sets are generated.

The experiment reported in this section was conducted on a Debian GNU/Linux 12 Work Station, ES-2670 v2 processors (20 physical cores, 40 logical processors, using up to 20 threads), 2.50 Ghz and 128Gb RAM. The Cplex (v22.1.1) Concert Technology library has been used, embedded in a C/C++ experimental code, for solving the decomposition submodels as well as for the straightforward solving of the full models; the default parameters are used unless explicitly mentioned. Additionally, a comparative study is realized between the straightforward using of the state-of-the-art solvers Cplex and Gurobi (v11.0.3). Given the problem-solving difficulty, the solver optimization is interrupted when reaching the wall time limit that has been imposed, 43200 seconds (12h).

Based on the scheme presented in Section 2 the procedure for ambiguity set generation is detailed for the instances in the experiment. The statistical manipulation of the data along this section has been carried out using the open source R statistical software, see [The R Project for Statistical Computing \(2024\)](#).

Taking into account the stochasticity of the second stage parameters that define the operations in the problem, they are classified in two groups with a predictably different and independent behaviour. The first group is composed of the commodity volume H_{mn}^ω to be consolidated in the CD entity from origin node m to destination node n ; the Normal, Weibull, Gamma and Lognormal distributions, say $q = 1, 2, 3, 4$, are considered to generate the different perturbations. The second group is composed of the capacity disruption fraction of the strip and stack doors D_i^ω and D_j^ω , respectively, where the uniform distribution is considered. Notice that the inbound volume to entering the CD entity and the outbound volume to exiting from, say S_m^ω and R_n^ω , respectively, are directly obtained from H_{mn}^ω , see Appendix A in the supplementary file. Additionally, the commodity handling and transportation cost G_{minj}^ω is also obtained from that H -parameter.

The appendices C, D and E, also in the supplementary file, show the results of the ambiguity set generation that is proposed as well as some other relevant results of the experiment. On the other hand, the main ND statistics as well as the original data are available from the authors under reasonable request.

5.1 Instance I1

5.1.1 I1. On ambiguity set \mathcal{P} generation

The smallest instance in the experiment is composed of 8 origins and 8 destinations, and 4 strip doors and 4 stack ones. In particular, ND is defined by a set of $|\Omega| = 5$ equiprobable scenarios, where the four strip and stack doors have not capacity disruptions (i.e., $D_i^\omega = D_j^\omega = 0 \forall \omega \in \Omega$). Let $|\mathcal{L}| = 1$ group of scenarios and $|\mathcal{H}| = 17$ parameters out of the 64 possible ones. The related non-zero realizations (i.e., commodity volumes H_{mn}^ω) are chosen *at random*, for scenario $\omega \in \Omega$ in ND. Let $\{\hat{\xi}_h^\omega \forall h \in \mathcal{H}^{\ell(\omega)}\}$ denote the set of realizations $\{H_{mn}^\omega\}$. On the other hand, hand, $|\mathcal{G}| = 1$ and, then, the PDs in set \mathcal{Q} can be followed by any uncertain parameter.

Based on the ϵ -perturbations vector of *cdf* in the assumed PDs for the ND uncertain parameters'

realizations, the candidate ambiguity set, for $\epsilon^\omega \sim N(0, \sigma_\epsilon^2)$ with $\sigma_\epsilon = 0.05$, is composed of the uncertain parameters' realizations ξ_h^ω , for $h \in \mathcal{H}$, $\omega \in \Omega_p$, $p \in \mathcal{P}'_q$, $q \in \mathcal{Q}$, where $\Omega = \Omega_p$, $|\mathcal{P}'_q| = 20$ for $q \in \mathcal{Q}$, $|\mathcal{Q}| = 4$; see the scheme presented in Section 2. Given the independency assumption of the parameters in \mathcal{H} and, then, the realizations' vector $(\xi_h^\omega \forall h \in \mathcal{H}^{\ell(\omega)})$ under scenario $\omega \in \Omega_p$ in perturbation p , it results that the likelihood associated with scenario ω allows to compute the weights $\{w^\omega\}$ as expression (1). Once those elements are computed as well as the distance matrices between ξ_h^ω and $\hat{\xi}_h^\omega$, the $|\mathcal{P}'_q| \times |\mathcal{Q}| = 80$ 'transportation' models (2) are solved to retrieve *proximity* ℓ_p^ρ , for $\rho = 2$, $p \in \mathcal{P}'_q$, $q \in \mathcal{Q}$.

Table 1 summarises the statistics as the first 5-centile and the first decile for the set of the 80 *proximities* in the experiment, based on the frequency distribution of ℓ_p^ρ as shown in Table C.1 in Appendix C.

Table 1: Instance I1. Statistics for the candidates to the ambiguity set

<i>Min</i>	<i>1st5cent</i>	<i>1st10cent</i>	<i>1stQu</i>	<i>Median</i>	<i>Mean</i>	<i>3rdQu</i>	<i>Max</i>
8.855	9.145	9.338	10.048	10.411	10.545	11.037	12.570

The *radius* θ to be satisfied by ℓ_p^ρ of any ambiguity set member p , for $p \in \mathcal{P}$, is a modeler-driven parameter. In case that it is the first decile $\theta_{10\%} = 9.338$, then the cardinality of the ambiguity is $|\mathcal{P}_{10\%}| = 8$. On the other hand, it is reduced to $|\mathcal{P}_{5\%}| = 4$ for the first 5-centile $\theta_{5\%} = 9.145$, where $\mathcal{P}_{5\%} \subset \mathcal{P}_{10\%}$.

Table 2 shows the dimensions of models LIP-RN (3) and LIP-SD (13), the solution value and the wall time required by the straightforward use of the solvers Cplex and Gurobi. The ambiguity sets \mathcal{P} under consideration are $\mathcal{P}_{5\%}$ and $\mathcal{P}_{10\%}$. The headings are as follows. *Inst-|P|*, instance code, where the ambiguity set cardinality is included; *m*, *n01*, *nc* and *nz*, number of constraints, binary variables, continuous variables and nonzero constraint matrix element, respectively. z^* , optimal solution cost; t_{cpx} and t_{grb} , wall time (seconds) required for obtaining z^* by solvers Cplex and Gurobi, respectively.

Table 2: Instance I1. CDDP models LIP-RN (3) and LIP-SD (13): Dimensions and Cplex and Gurobi results

Note: *: 0.03% optimality gap

<i>Inst- P </i>	<i>m</i>	<i>n01</i>	<i>nc</i>	<i>nz</i>	z^*	t_{cpx}	t_{grb}
I1-RN-4	13634	1680	32021	98398	7260.56	856	353
I1-SD-4	13735	1684	32065	99606	7459.31	712	3062
I1-RN-8	27258	3320	64041	196717	7260.56	37739	6225
I1-SD-8	27459	3328	64129	199138	7462.36	6365	42000*

5.1.2 I1. Solution of model LIP-RN (3) for ambiguity set $\mathcal{P}_{5\%}$

The optimal solution cost, say, $z^* = u = 7260.56$ is composed of the first stage entity building cost $\hat{C} = 1538$ (4c) and the second stage expected cost 5722.56. Table C.2 in Appendix C shows the weights and the CD node-door assignment cost \hat{F}^ω (4d) under the scenarios $\{\omega\}$ in the ambiguity set members. There are six black swan scenarios.

5.1.3 I1. Solution of model LIP-SD (13) for ambiguity set $\mathcal{P}_{5\%}$

The aim is to prevent the outsourcing costs as retrieved from the optimal solution of model LIP-RN (3). For that purpose an appropriate modeler-driven triplet (cost threshold, upper bound cost surplus and upper bound on the expected surplus cost in the scenarios) should be considered in model LIP-SD (13), see Appendix C. It can be observed in the solution shown in Table C.3 that there is not outsourcing in any black swan scenario at the price of a reasonable cost z_{SD}^* . On the other hand, it can also be observed that the constraints (12b) and (12c) are satisfied.

5.1.4 I1. Solution of model LIP-RN (3) for ambiguity set $\mathcal{P}_{10\%}$

The optimal solution cost, say, $z_{RN}^* = u = 7260.56$ is the same as for ambiguity $\mathcal{P}_{5\%}$. Notice that the setting is robust optimization and, on the other hand, $\mathcal{P}_{5\%} \subset \mathcal{P}_{10\%}$. As a matter of fact there are in total eleven (black swan) scenarios in the ambiguity set members which outsourcing cost has a high variability, so that it varies from 7602812 to 14000288.

5.1.5 I1. Solution of model LIP-SD (13) for ambiguity $\mathcal{P}_{10\%}$

The aim is to prevent the outsourcing costs as retrieved from the optimal solution of model LIP-RN (3). The experiment is similar to the one considered for set $\mathcal{P}_{5\%}$. The optimal cost is $z_{SD}^* = 7462.36$ (slightly higher than for ambiguity set $\mathcal{P}_{5\%}$, notice that the constraint system is more restricted), where there is not outsourcing any more in any black swan scenario.

5.1.6 I1. Comparison of ambiguity sets' solutions

Observed in Table 2 that the number of elements of instance I1 is relatively small. However, the RN and SD models' dimensions are certainly not; as a matter of fact, they are linearly increasing with the ambiguity set cardinality. Both solvers Cplex and Gurobi obtain the optimal DRO solution cost for each ambiguity set under consideration. Observe the variability of the wall time required by the solvers when dealing with the RN and SD model's versions for $|\mathcal{P}| = 8$. Notice that Cplex requires about 10h 29 minutes for solving I1-RN-8. On the other hand, Gurobi cannot prove the optimality for case I1-SD-8 in the 12h time limit, reporting a 0.03% gap, where it is 0.04% after 1384s. In any case, the SD solutions avoid outsourcing in the black swan scenarios without a high increase in the optimal cost.

The CDDP cost distribution in the instance is depicted in Fig. 3 for the members of the two ambiguity sets, $\mathcal{P}_{5\%}$ and $\mathcal{P}_{10\%}$, where $|\mathcal{P}_{5\%}| = 4$ and $|\mathcal{P}_{10\%}| = 8$. It is reported by using the boxplot technology, where it allows to display the summary of the distribution of the cost in the different models, being quantified with the following statistical measures: minimum, first quartile, median, third quartile, and maximum. The central box in each experiment spans from the first quartile to the third one, in an interquartile mode, the segment inside the rectangle shows the median cost, and the *whiskers* above and below the box show the minimum and maximum cost. The column for each DRO identifier depicts the cost distribution of the ambiguity set members that is retrieved from the solution of models LIP-RN and LIP-SD.

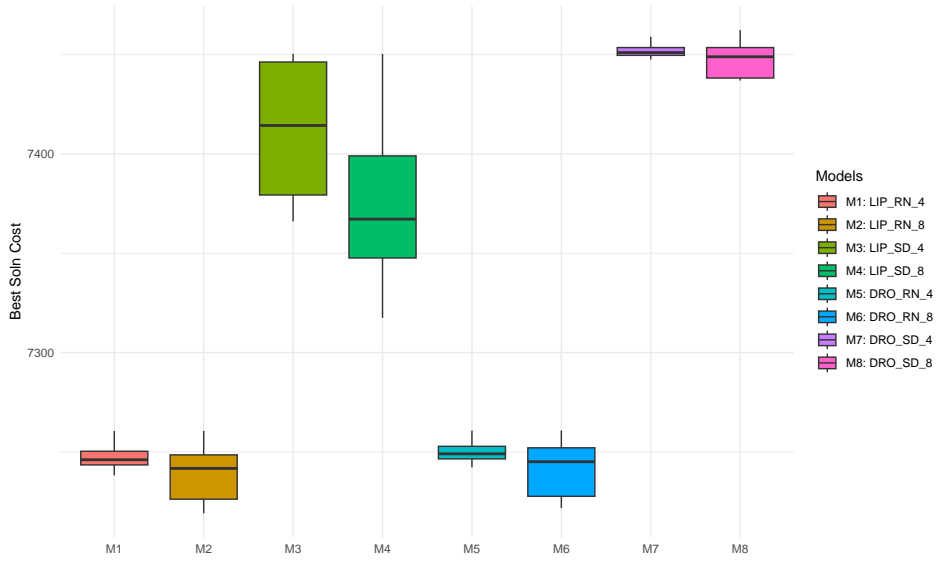


Figure 3: Instance I1. DRO cost distribution retrieved from the solution of models LIP-RN (3) and LIP-SD (13) in the ambiguity sets

5.2 Instance I3

5.2.1 I3. On ambiguity set \mathcal{P} generation

The instance is composed of 10 origins, 10 destinations, 5 strip doors and 5 stack ones. In particular, ND is defined by $|\Omega| = 10$ equiprobable scenarios in $|\mathcal{L}| = 2$ groups, say $|\Omega^1| = 5$ and $|\Omega^2| = 5$. Table 3 reports the dimensions of the sets in the instance. The headings are as follows for scenario group ℓ : $|\Omega^\ell|$, number of scenarios; $n\mathcal{M}$ (resp., $n\mathcal{N}$), number of origin (respectively, destination) nodes; $n\mathcal{I}$ (resp., $n\mathcal{J}$), number of strip (respectively, stack) doors; $m\mathcal{H}$, cardinality of the set of original uncertain parameters, i.e., $n\mathcal{M} \times n\mathcal{N}$; $|\mathcal{H}^\ell|$, number of uncertain parameters, such that it is taken *at random* in the range $(1, m\mathcal{H})$. Notice that the realizations of the $|\mathcal{H}^\ell|$ chosen parameters are also generated *at random*. On the other hand, $|\mathcal{G}| = 1$ and, then, the PDs in set \mathcal{Q} can be followed by any uncertain parameter.

Table 3: Instance I3. Dimensions of scenario groups in set \mathcal{L}

ℓ	$ \Omega^\ell $	$n\mathcal{M}$	$n\mathcal{N}$	$n\mathcal{I}$	$n\mathcal{J}$	$m\mathcal{H}$	$ \mathcal{H}^\ell $
1	5	8	8	4	4	64	17
2	5	10	10	5	5	100	26

It can be deduced from Table 3 that 5- $n\mathcal{I}$ and 5- $n\mathcal{J}$ *given* strip and stack doors, respectively, *are* fully disrupted for scenario group $\ell = 1$, while the other door *can* be partially or fully disrupted *at random*, if any. On the other hand, no *given* door *is* fully disrupted for scenario group $\ell = 2$. Notice that there are $|\mathcal{H}^1| = 17$ and $|\mathcal{H}^2| = 26$ parameters out of $m\mathcal{H} = 64$ and 100 possible ones, respectively. The related non-zero realizations (i.e., commodity volumes H_{mn}^ω) in ND are chosen *at random*, for each scenario ω in $\Omega^1 \cup \Omega^2$. On the other hand, $|\mathcal{G}| = 1$ and, then, the PDs in set \mathcal{Q} can be followed by any uncertain parameter.

Following the scheme presented in Section 2, the candidate ambiguity set is composed of the uncertain parameters' realizations ξ_h^ω , for \mathcal{H}^ℓ , $\omega \in \Omega^\ell$, $\ell = \{1, 2\}$, where $\Omega_p = \Omega$, for $p \in \mathcal{P}'_q$, $q \in \mathcal{Q}$, $|\Omega_p| = 10$, $|\mathcal{P}'_q| = 20$, $|\mathcal{Q}| = 4$. $|\mathcal{H}| = 38$, for $\mathcal{H} = \mathcal{H}^1 \cup \mathcal{H}^2$, since $\mathcal{H}^1 \cap \mathcal{H}^2 \neq \emptyset$; as a matter of fact there are 5 parameters' repetitions.

Table 4 summarises some statistics as the first 3-centile and the first 7-centile for the set of the 80 *proximities* in the experiment, based on the ℓ_p^ρ frequency distribution as shown in Table D.4 in Appendix D. Those statistics are retrieved from the solution of the 'transportation' models (2). Recall that those models are solved once the parameters' realizations are generated for each of the four chosen PD in set \mathcal{Q} and the distance matrices are computed between those realizations in each candidate ambiguity set member and the ND ones.

Table 4: Instance I3. Statistics for the candidates to the ambiguity set

<i>Min</i>	<i>1st3cent</i>	<i>1st7cent</i>	<i>1stQu</i>	<i>Median</i>	<i>Mean</i>	<i>3rdQu</i>	<i>Max</i>
9.91	10.31	10.61	10.99	11.57	11.68	12.34	14.17

In case that the *radius* is the first 7-centile $\theta_{7\%} = 10.61$, the cardinality of the ambiguity set is $|\mathcal{P}_{7\%}| = 6$. On the other hand, it is reduced to $|\mathcal{P}_{3\%}| = 3$ for the first 3-centile $\theta_{5\%} = 10.31$, where $\mathcal{P}_{3\%} \subset \mathcal{P}_{7\%}$.

5.2.2 I3. On solving models LIP-RN (3) and LIP-SD (13)

Table 5 shows the model dimensions of LIP-RN (3) and LIP-SD (13) as well as the main computational results and wall time required by the straightforward use of solvers Cplex and Gurobi. Notice that the dimensions are approximately double than the ones of instance I1. The ambiguity sets \mathcal{P} under consideration are $\mathcal{P}_{3\%}$ and $\mathcal{P}_{7\%}$. The new headings are as follows. \underline{z}_L , LP lower bound of the optimal

solution cost; $\underline{t}_{\bullet-L}$, \bar{z}_{\bullet} and GAP_{\bullet} , wall time required for obtaining the LP lower bound, incumbent cost and optimality gap, respectively, provided by solver \bullet , where $\bullet \in \{cpx, grb\}$. It is worth to point out that the lower bound \underline{z}_L is obtained by solving the model attached to the root node in the B&C phase; \underline{t}_{cpx-L} gives the wall time required by Cplex and \underline{t}_{grb-L} does it by Gurobi for the automatically selected barrier method just before executing the crossover phase.

Table 5: Instance I3. CDDP models LIP-RN (3) and LIP-SD (13): Dimensions and Cplex and Gurobi results

$Inst- \mathcal{P} $	m	$n01$	nc	nz	\underline{z}_L	\underline{t}_{cpx-L}	\bar{z}_{cpx}	GAP_{cpx}	\underline{t}_{grb-L}	\bar{z}_{grb}	GAP_{grb}
I3-RN-3	28995	3110	78031	230823	7984.59	3	8451.89	5.5	20	8339.79	4.3
I3-SD-3	29131	3113	78094	232813	8198.65	2	8526.87	3.8	6	8503.66	3.6
I3-RN-6	57978	6170	156061	461546	7991.35	7	8597.93	7.0	229	8315.29	3.9
I3-SD-6	58249	6176	156187	465526	8230.65	9	8695.13	5.3	23	8512.42	3.3

The first observation is that the models are very difficult to solve; as a matter of fact, they cannot be solved up to optimality in the given time limit. Notice the small time required by both solvers for obtaining the LP bound \underline{z}_L versus the 12h time limit that is reached while solving the rest of nodes in the B&C phase, see Table 5. It is also worth to observe that both solvers provide the *same* LP bound in spite of their potentially different preprocessing approaches. The optimality GAP is expressed as $100 \cdot \frac{\bar{z} - \underline{z}}{\bar{z}}$, as typically done in the commercial solvers, where \bar{z} is the incumbent cost and \underline{z} is the smallest cost of the solutions retrieved from the submodels in the set of active B&C nodes at the optimization's interruption. It can be observed that GAP_{grb} is smaller than GAP_{cpx} , mainly for $|\mathcal{P}| = 6$. Additionally, notice that the SD-incumbent cost is higher than the RN-incumbent one.

The weights and the CD node-door assignment cost under the scenarios in the ambiguity set $\mathcal{P}_{3\%}$, retrieved from the solution of model LIP-RN (3) are presented in Table D.5 in Appendix D. Notice that there ten several black swan scenarios with high costs (due to outsourcing) in the three ambiguity set members, sharing as well a very small weight. The outsourcing costs can be prevented by considering an appropriate modeler-driven SD parameters' triplet, see Appendix D. Table D.6 shows some results retrieved from the incumbent solution of model LIP-SD (13) to be compared with the RN solution. It can be seen that the black swan scenarios have not, any more, so negative implications in the SD solution obtained by both solvers at the price of a reasonable cost increase. The rationale presented above for ambiguity set $\mathcal{P}_{3\%}$ is similarly followed for $\mathcal{P}_{7\%}$.

Fig. 4 depicts, with the same meaning as Fig. 3, a comparison of the CDDP cost distribution of the ambiguity set members that is retrieved from the solution of models LIP-RN and LIP-SD in the two ambiguity sets $\mathcal{P}_{3\%}$ and $\mathcal{P}_{7\%}$, where $|\mathcal{P}_{3\%}| = 3$ and $|\mathcal{P}_{7\%}| = 6$, and the DRO identifiers M1 and M11 refer to the matheuristic solution, see Section 5.4.

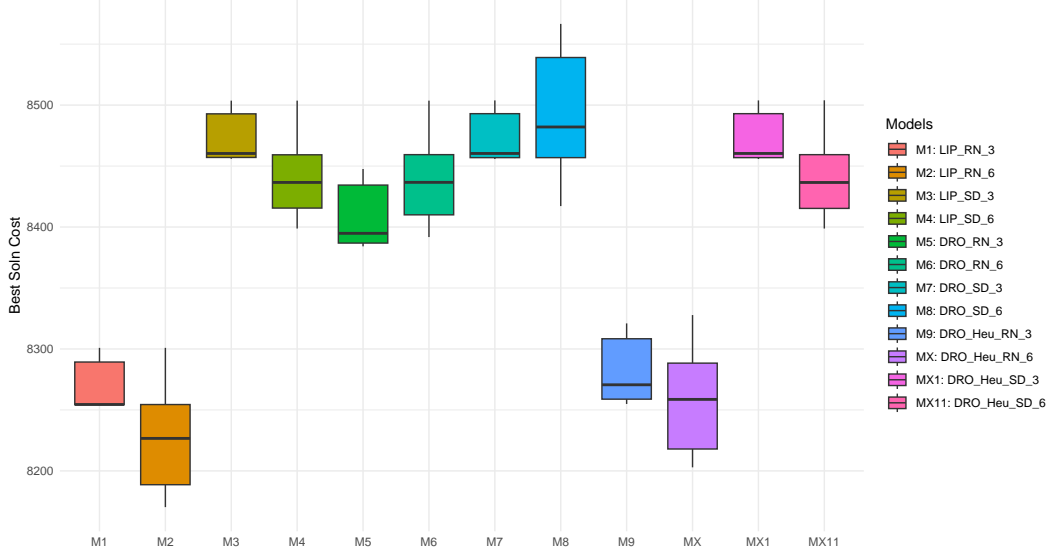


Figure 4: Instance I3. DRO cost distribution retrieved from the solution of models LIP-RN (3) and LIP-SD (13) in the ambiguity sets

5.3 Instance I7

5.3.1 I7. On ambiguity set \mathcal{P} generation

The instance is composed of 20 origins, 20 destinations, 10 strip doors and 10 stack ones. In particular, ND is defined by $|\Omega| = 20$ equiprobable scenarios in $|\mathcal{L}| = 4$ groups. Table 6 reports the dimensions of the sets in the instance. It can be deduced from the table that 10- $n\mathcal{I}$ and 10- $n\mathcal{J}$ *given* strip and stack doors, respectively, *are* fully disrupted for each scenario group, while the other doors *can* be partially or fully disrupted *at random*, if any. So, obviously, no *given* door *is* fully disrupted for scenario group $\ell = 4$.

Table 6: Instance I7. Dimensions of scenario groups in set \mathcal{L}

ℓ	$ \Omega^\ell $	$n\mathcal{M}$	$n\mathcal{N}$	$n\mathcal{I}$	$n\mathcal{J}$	$m\mathcal{H}$	$ \mathcal{H}^\ell $
1	5	8	8	4	4	64	17
2	5	10	10	5	5	100	26
3	5	15	15	6	6	225	57
4	5	20	20	10	10	400	101

Following the scheme presented in Section 2, the candidate ambiguity set is composed of the uncertain parameters' realizations ξ_h^ω , for $h \in \mathcal{H}^\ell$, $\omega \in \Omega^\ell$, $\ell \in \mathcal{L}$, where $\Omega_p = \bigcup_{\ell \in \mathcal{L}} \Omega^\ell$, for $p \in \mathcal{P}'_q$, $q \in \mathcal{Q}$, $|\Omega_p| = 20$, $|\mathcal{P}'_q| = 20$, $|\mathcal{Q}| = 4$. On the other hand, $|\mathcal{H}| = 169$, $\mathcal{H} = \bigcup_{l=1}^4 \mathcal{H}^l$, where there are $\sum_{l=1}^4 |\mathcal{H}^l| - |\mathcal{H}| = 32$ parameters' repetitions.

Table 7 summarises some statistics as the first 3-centile and the first 7-centile for the set of 80

proximities in the experiment, based on the frequency distribution of ℓ_p as shown in Table E.9 in Appendix E. Those statistics are retrieved from the solution of the 'transportation' models (2).

Table 7: Instance I7. Statistics for the candidates to the ambiguity set

<i>Min</i>	<i>1st3cent</i>	<i>1st7cent</i>	<i>1stQu</i>	<i>Median</i>	<i>Mean</i>	<i>3rdQu</i>	<i>Max</i>
11.80	12.29	12.58	13.30	13.85	13.93	14.40	17.53

In case that the *radius* is the first 7-centile $\theta_{7\%} = 12.58$, the cardinality of the ambiguity set is $|\mathcal{P}_{7\%}| = 6$. On the other hand, it is reduced to $|\mathcal{P}_{3\%}| = 3$ for the first 3-centile $\theta_{3\%} = 12.29$, where $\mathcal{P}_{3\%} \subset \mathcal{P}_{7\%}$.

5.3.2 I7. On solving models LIP-RN (3) and LIP-SD (13)

Table 8 shows the model dimensions for LIP-RN (3) and LIP-SD (13) as well as the main computational results. Notice that the dimensions are one order of magnitude higher than the ones of instance I3. So, the models are much more difficult to solve and, then, the optimization also reaches the time limit (12h). It can be observed that the Cplex solution for the RN version is very bad, it has been obtained in the solver's preprocessing; it is worthless to this respect. On the other hand, the solution provided by Gurobi for the RN model is an acceptable one; observe the small time required by the barrier method for obtaining the LP value without using the crossover scheme, since otherwise the time would be one order of magnitude higher.

It is worth to point out that none of the two state-of-the-art solvers could find any feasible solution in the 12h wall time limit for the SD models. Cplex is even unable to provide an LP bound for the largest instance I7-SD-6.

Table 8: Instance I7. CDDP models LIP-RN (3) and LIP-SD (13): Dimensions, and Cplex and Gurobi results

Note: —, No feas soln found

<i>Inst- P </i>	<i>m</i>	<i>n01</i>	<i>nc</i>	<i>nz</i>	\bar{z}_L	\underline{t}_{cpx-L}	\bar{z}_{cpx}	GAP_{cpx}	\underline{t}_{grb-L}	\bar{z}_{grb}	GAP_{grb}
I7-RN-3	210865	12970	969436	2568280	20723.10	304	32419500	99.94	220	23394.69	11.4
I7-SD-3	211121	12973	969559	2575214	20947.13	26844	—	—	130	—	—
I7-RN-6	421708	25840	1938871	5136361	21612.95	233	41457800	99.94	205	24224.44	10.8
I7-SD-6	422219	25486	1939479	5150231	21612.95	—	—	—	244	—	—

It can be deducted from the results shown in Tables 5 and 8 that Gurobi 11.0.3 outperforms Cplex 22.1.1 whenever a feasible solution is found.

5.4 Matheuristic performance

The performance of the matheuristic introduced in Sections 3.4 and 4.3 is analyzed in this section for the RN and SD risk measures, respectively. For that purpose, the difficult instances I3 and I7 are considered, which problem dimensions are shown in Tables 3 and 6, respectively. On the other hand, the dimensions of models LIP-RN (3) and LIP-SD (13) are shown in the related Tables 5 and 8.

Table 9 shows the main results, which headings are as follows: \underline{z}_L , LP lower bound of the optimal solution cost taken from Tables 5 and 8; \underline{z}_H , lower bound obtained by the matheuristic expressed as \underline{z}_{RN} (8) for RN case and \underline{z}_{SD} (17) for SD one; \underline{t}_L and \underline{t}_H , related wall times; $\hat{C}_{1,H}$ and \hat{F}_H , first stage cost and second stage expected one (the latter expressed as $\sum_{\omega \in \Omega_p} w^\omega \hat{F}^{c,\omega}$), respectively, that compose the total cost \bar{z}_H of the incumbent solution (say, \bar{z}_{RN} (9) for RN and \bar{z}_{SD} (18) for SD); \bar{t}_H , wall time required by \bar{z}_H , where time \underline{t}_H has been added; $GAP_H\%$, optimality gap of the incumbent cost to be expressed as $100 \cdot \frac{\bar{z}_H - \underline{z}'}{\bar{z}_H}$, in the spirit of the solvers, where $\underline{z}' = \max\{\underline{z}_L, \underline{z}_H\}$; and GR_H , goodness ratio of cost \bar{z}_H with respect to the Gurobi incumbent cost \bar{z}_{grb} . It is worth to point out that $\underline{z}' = \underline{z}_H$ for I3-SD-3 and I3-RN-6, otherwise, $\underline{z}' = \underline{z}_L$.

Anyway it is remarkable the usefulness of the set of the alternative fixings of the first stage variables for obtaining the incumbent solution cost \bar{z}_H , given the wall time, optimality gap and goodness ratio as shown in Table 9. Notice that those fixings are retrieved from the solutions obtained in the SCD-based lower bound approaches, see Sections 3.4 for RN and 4.3 for SD.

Table 9: Instances I3 and I7. CDDP models LIP-RN (3) and LIP-SD (13): Matheuristic results

$Inst- P $	\underline{z}_L	\underline{t}_L	\underline{z}_H	\underline{t}_H	\bar{z}_H	\bar{t}_H	$\hat{C}_{1,H}$	\hat{F}_H	GAP_H	GR_H
I3-RN-3	7984.59	20	6456.43	32	8320.96	161	1849	6471.96	4.04	0.998
I3-SD-3	8198.65	6	8226.63	360	8503.66	402	2082	6421.66	3.26	1.000
I3-RN-6	7991.35	229	8130.70	234	8327.80	564	1849	6478.80	2.37	1.001
I3-SD-6	8230.65	220	8226.63	636	8503.94	793	2089	6414.94	3.21	0.999
I7-RN-3	20723.10	220	17418.44	14400	22402.18	14787	7157	15245.18	7.49	0.957
I7-SD-3	20947.13	123	19435.35	14400	22402.69	14876	7284	15118.69	6.49	∞
I7-RN-6	21612.95	205	20078.54	14400	23700.67	14875	7784	15916.67	8.81	0.971
I7-SD-6	21612.95	206	20729.06	14400	23939.31	14845	8023	15916.31	9.71	∞

Tables D.7 and D.8 in Appendix D show similar types of results for instance I3 as those shown in Table D.6 while solved by straightforward use of the two commercial solvers. Additionally, similar observations can be made on the results retrieved from the solutions of models LIP-RN (3) and LIP-SD (13) for instance I7 as shown in Tables E.10 and E.11. Notice that the black swan scenarios have outsourcing in the RN solutions for the four instances I3-RN-3, I3-RN-6, I7-RN-3 and I7-RN-6. On the other hand, it is also remarkable that the SD solutions have not outsourcing any more and, additionally, the SD bounds \bar{s}^1 in (12b) and \bar{s}^{-1} in (12c) are satisfied for the four instances I3-SD-3, I3-SD-6, I7-SD-3 and I7-SD-6.

Parallelism. It is worth to remark the embarrassing parallelism on obtaining the bounds provided by the matheuristic. Notice that the lower bounds (8) for RN and (17) for SD are obtained by independently

solving $|\mathcal{C}|$ submodels (7) for RN and (16) for SD as well as the LP relaxation of the related models (3) and (13). Since those executions can be performed in parallel, let \underline{t}_H be the highest wall time for solving the most demanding related submodels (7) for RN and (16) for SD. In a similar way, the upper bounds (9) for RN and (18) for SD are obtained by independently solving $|\mathcal{C}| \times |\mathcal{P}|$ 'restricted' submodels (3) and (13), respectively, that result for the appropriate fixing of the first stage variables. Those submodels are solved by considering the matheuristic algorithm so-named SCS4B presented in Escudero et al. (2024b) for CDDP-TS problems. So, the executions can be performed in parallel, then let \bar{t}_H be the highest wall time for solving the most demanding related 'restricted' submodels (3) and (13) for the RN and SD risk measures, respectively, where \underline{t}_H is added. Note: The time limit for solving each of the submodels is set up to 4h.

6 Conclusions and future research agenda

A two-stage DRO model and related mathematically equivalent MILP formulation have been introduced for the NP-hard quadratic CD design problem under uncertainty. It has broad applicability and it is extremely difficult to solve. Its main elements are as follows:

1. A ND is given for representing the uncertainty of the main parameters and the related sets. However, the truly PD followed the those parameters is assumed to be unknown.
2. A scheme for generating ambiguity sets is proposed.
3. Given the potential high variability of that uncertainty, a second-order SD risk averse functional is introduced (by considering quadratic functions) as a counterpart of its RN version.

The procedure for generating candidate ambiguity set members is based on a perturbation scheme for each given PD, where ND is potentially assumed to coming from. The ambiguity set members to be selected from the candidate one in order to consider them in the DRO model depends on the *proximity* value of their Wasserstein distances to ND.

The testbed in the computational experiment is composed of small-medium, medium- and large-sized instances, to be named as I1-, I3- and I7-types, where the number of uncertain parameters is 17, 43 and 201, respectively. Twenty perturbation-based candidate members are generated for each of the four PDs under consideration in each instance. So, eighty Wasserstein transportation models are optimized for selecting two ambiguity sets in each instance, which cardinality varies from 3 to 8. The scenario sets considered in the ambiguity set members have a cardinality that varies from 5 to 20. The resulting MILP models for CDDP are I1-RN- $|\mathcal{P}|$ and I1-SD- $|\mathcal{P}|$ for $|\mathcal{P}| = 4, 8$, I3-RN- $|\mathcal{P}|$ and I3-SD- $|\mathcal{P}|$ for $|\mathcal{P}| = 3, 6$, and I7-RN- $|\mathcal{P}|$ and I7-SD- $|\mathcal{P}|$ for $|\mathcal{P}| = 3, 6$, where $|\mathcal{P}|$ is the cardinality of the ambiguity set. The dimensions are up to 420,000+ constraints, 25,000+ binary variables and 1,900,000+ continuous ones with very complex combinatorial structures.

A computational comparison between the straightforward use of the state-of-the-art solvers Cplex and Gurobi is performed by considering the RN and SD versions. For medium- and large-sized RN instances, Gurobi is the winner. It always provides feasible solutions, but reaching the 12h wall time limit without proving the incumbent DRO solution’s optimality in most of the runs for the instances. In any case, its quasi-optimality gap is up to 11.4% for RN, and none of those solvers can provide any feasible solution for the large-sized SD instances.

As an alternative to the straightforward use of the MILP solvers, a *min-max* matheuristic approach is introduced for problem-solving. It takes benefit of the CDDP structures that are embedded in the RN and SD versions of the original two-stage CDDP-DRO model. Interestingly, the proposal provides an incumbent solution for all tested runs in a very reasonable wall time; its optimality GAP is ranging from 2.37 to 9.71%. Additionally, the goodness ratio of the solution costs’ proposal versus the Gurobi’s one is ranging from 0.957 to 1.001, for the runs where the latter provides a solution.

6.1 Main items in the future research agenda

1. Generalization of the matheuristic algorithm proposed in this work to solve general two-stage DRO MILP problems.
2. A multi-horizon DRO MBQ approach is to be considered for the RN and SD versions of the CD door design problem.

Acknowledgments

The authors wish to express their thanks to Antonio Alonso-Ayuso, Juan Francisco Monge, Domingo Morales and Leandro Pardo for fruitful discussions on the ambiguity set generation and modeling. This research has been partially supported by the projects RTI2018-094269-B-I00 and PID2021-122640OB-I00 (L.F. Escudero), Grant PID2023-147410NB-100 funded by MCIN/AEI/ 10.13039/501100011033 and by ERDF/EU and Grupo de Investigación EOPT (IT-1494-22) from the Basque Government (M.A. Garín and A. Unzueta).

References

- Akkerman, F., Lalla-Ruiz, E., Mes, M. & Spitters, T. (2022). Cross-docking: Current research versus industry practice and industry 4.0 adoption. In Bondarouk, T. and Olivas-Luján, M.R. (Eds.). *Smart Industry - Better Management*, 69-104, Emerald Group Holdings Co.
- Altaf, A., El Amraoui, A., Delmotte, F. & Lecoutre, C. (2025). Robust cross-dock assignment problem with uncertain cost parameters. *International Journal of Production Research*, 1–26, doi.org/10.1080/00207543.2025.2469164

- Ardakani, A. & Fei, J. (2020). A systematic literature review on uncertainties in cross-docking operations. *Modern Supply Chain Research and Applications*, doi: 10.1108/MS CRA-04-2019-0011.
- Artzner, P., Delbaen, F., Eber, J.M. & Heath, D. (1999). Coherent measures of risk. *Mathematical Finance*, 9:203-228.
- Asgharyar, M., Farmand, N. & Shetab-Boushehri, S.N. (2025). A novel mathematical modeling approach for integrating a periodic vehicle routing problem and cross-docking system *Computers & Operations Research*, 107048, doi.org/10.1016/j.cor.2025.107048.
- Bayraksan, G., Maggioni, F., Faccini, D. & Yang, M. (2024). Bounds for multistage mixed-integer distributionally robust optimization. *SIAM Journal on Optimization*, 34:682-717.
- van Beesten E.R., Romeijnnders, W. & Morton, D.P. (2024). Pragmatic distributionally robust optimization for simple integer recourse models. *SIAM Journal on Optimization*, 34:1755-1783.
- Bertsimas, D., McCord, C. & Sturt, B. (2023). Dynamic optimization with side information. *European Journal of Operational Research*, 304:634-651.
- Bertsimas, D., Shtern, D. & Sturt, B. (2022). A data-driven approach to multi-stage stochastic linear optimization. *Management Science*, 69:51-74.
- Boysen, N. & Flidner, M. (2010). Cross-dock scheduling: classification, literature review and research agenda. *Omega*, 38:423-422.
- Buakum, D & Wisittipanich, W. (2019). A literature review and further research direction in cross-docking. Proceedings of the International Conference on Industrial Engineering and Operations Management. Bangkok, Thailand.
- Caunhye, A.M. & Alem, D. (2023). Practicable robust stochastic optimization under divergence measures with an application to equitable humanitarian response planning. *OR Spectrum*, 45:759-806.
- Cesarone, F. & Puerto, J. (2025). Flexible enhanced indexation models through stochastic dominance and ordered weighted average optimization. *European Journal of Operational Research*, 323:657-670.
- Chargui, T., Essghaier, F., Bekrar, A., Allaoui, H., Trentesaux, D., Goncalves, G. (2021). Multi-objective cross-docking in physical internet hubs under arrival time uncertainty. In: Borangiu, T., Trentesaux, D., Leitão, P., Cardin, O., Lamouri, S. (eds). *Service Oriented, Holonic and Multi-Agent Manufacturing Systems for Industry of the Future*. Studies in Computational Intelligence, vol 952. Springer.
- Dentcheva, D. & Ruszczyński, A. (2003). Optimization with stochastic dominance constraints. *SIAM Journal on Optimization*, 14:548-566.
- Dentcheva, D. & Ruszczyński, A. (2010). A robust stochastic dominance and its application to the risk averse optimization. *Mathematical Programming*, 123:85-100.
- Dentcheva, D. & Ruszczyński, A. (2024). Numerical methods for problems with stochastic dominance constraints. In: *Risk-Averse Optimization and Control*. Springer.
- Dentcheva, D. & Yi, Y. (2025). Relaxation of stochastic dominance constraint via optimal transport. *SIAM Journal on Optimization*, submitted.
- Duque, D., Mehrotra, S. & Morton, D.P. (2022) Distributionally robust two-stage stochastic programming. *SIAM Journal on Optimization*, 32:1499-1522.

- El Tonbari, M., Nemhauser, G. & Toriello A. (2024). Distributionally robust disaster relief planning under the Wasserstein set. *Computers & Operations Research*, 168:106689.
- Erdogan, E. & Iyengar, G. (2006). Ambiguous chance-constrained problems and robust optimization. *Mathematical Programming*, 107:37-61.
- Escudero, L.F., Garín, A., Monge, J.F. & Unzueta, A. (2020). Some matheuristic algorithms for multistage stochastic optimization models with endogenous uncertainty and risk management. *European Journal of Operational Research*, 285:988-1001.
- Escudero, L.F., Garín, A. & Unzueta, A. (2016). Cluster Lagrangean decomposition in multistage stochastic optimization. *Computers & Operations Research*, 67:48-62.
- Escudero, L.F., Garín, M.A. & Unzueta, A. (2024a). On solving the Cross-dock Door Assignment Problem, CDAP. *International Journal of Production Research*, 64, 1262-1276.
- Escudero, L.F., Garín, M.A. & Unzueta, A. (2024b). A methodology for the cross-dock door platforms design under uncertainty. *arXiv:arXiv:2403.03686*.
- Escudero, L.F. & Monge, J.F. (2018). On capacity expansion planning under strategic and operational uncertainties based on stochastic dominance risk averse management. *Computational Management Science*, 15:479-500.
- Escudero, L.F. & Monge, J.F. (2023). On risk management of multistage multiscale FLP under uncertainty. Chapter in Eiselt, H.A. & Marianov, V. (eds.), *Uncertainty in facility location models*. International series in Operations Research & Management Sciences, 437, pp.355-390, Springer.
- Esfahani, P.M. & Kuhn, D. (2015). Data-driven distributionally robust optimization using the Wasserstein metric: performance guarantees and tractable reformulations. *arXiv:arXiv:1505.05116*.
- Essghaier, F., Allaoui, H. & Goncalves, G. (2021). Truck to door assignment on a shared cross-dock under uncertainty. *Expert Systems with Applications* 182:114889.
- Fonseca, G.B., Nogueira, T.H. & Ravetti, M.G. (2024). Stability approach to CDC truck scheduling problem under uncertainty. *Optimization Letters*, doi.org/10.1007/s11590-024-02137-6.
- Fortet, R. (1960). Application de l'algèbre de boole en recherche operationelle. *Revue Française de Recherche Operationelle*, 4:17-26.
- Gallo, A., Accorsi, R., Akkerman, R. & Manzini, R. (2022). Scheduling cross-docking operations under uncertainty: A stochastic genetic algorithm based on scenarios tree. *EURO Journal on Transportation and Logistics*, 11:100095
- Gao, R. & Kleywegt, A.J. (2022). Distributionally robust stochastic optimization with Wasserstein distance. *Mathematics of Operations Research*, 48:603-655. Previously, ArXiv:1604.02199v2, 2016.
- Ghaoui, L.F., Oks, M. & Oustry, F. (2003). Worst case value-at-risk and robust portfolio optimization. A conic programming approach. *Operations Research*, 51:543-556.
- Gelareh, S., Glover, F., Guemri, O., Hanafi, S., Nduwayo, P. & Todosijevic, R. (2020). A comparative study of formulations for a cross-dock door assignment problem. *Omega*, 91:10215.
- Gollmer, R., Gotzes, Y. & Schultz, R. (2011). A note on second-order stochastic dominance constraints induced by mixed-integer linear recourse. *Mathematical Programming*, 126:179-190.

- Goodarzi, A.H., Zegordi, S.H., Alpan, G., Kamalabadi, I.N. & Kashan, A.H. (2020). Reliable cross-docking location problem under the risk of disruptions. *Operational Research*, doi.org/10.1007/s12351-020-00583-5.
- Guignard, M., Hahn, P.M., Pessoa, A.A., and Cardoso da Silva, D. 2012. Algorithms for the Cross-dock Door Assignment Problem. *In Proceedings of the Fourth International Workshop on Model-Based Metaheuristics 2012*. www.optimization-online.org/DB-FILE/2012/06/3509.pdf.
- Guignard, M. 2020. Strong RLT1 bounds from decomposable Lagrangean Relaxation for some quadratic 0–1 optimization problems with linear constraints. *Annals of Operations Research*, 286: 173–200.
- HoNguyen, N. & Wright, S. (2023). Adversarial classification via distributional robustness with Wasserstein ambiguity. *Mathematical Programming*, 198:1411-1447.
- Hosseini-Nodeh, Z., Khanjani-Shiraz, R. & Pardalos, P.M. (2022). Distributionally Robust Portfolio Optimization with Second-Order Stochastic Dominance Based on Wasserstein Metric. *Information Sciences*, doi.org/10.1016/j.ins.2022.09.039.
- Huong, D., Zhu, S., Fabozzi, F.J. & Fukushima, M. (2008). Robust portfolio selection with uncertain exit time: A robust CVaR approach. *Journal of Economic Dynamics & Control*, 32:594-623.
- Jiang, S., Liu, Q., Wu, L., Zhang, Y., Deveci, M. & Chen, Z.-S. (2024). A distributionally robust optimization approach for the potassium fertilizer product transportation considering transshipment through crossdocks. *Computers & Operations Research*, 171:106788.
- Kantorovich, L.V. (1942). On the Translocation of Masses. *Doklady Akad. Nauk SSSR*, 37:199-201. An English translation in *Management Science*, 5:1-4, 1958.
- Kiani Mavi, R., Goh, M., Kiani Mavi, N., Jie, F., Brown, K., Biermann, S. & Khanfar, A. 2020. Cross-Docking: a systematic literature review. *Sustainability*, 12:4789; doi: 10.3390/su12114789.
- Knight, F.H. (2012). Risk, uncertainty and profit. *Courier Corporation*. Original edition, 1921, Houghton Miffling.
- McCormick, G.P. (1976). Computability of global solutions to factorable nonconvex programs: Part I — Convex underestimating problems. *Mathematical Programming*, 10:147-175.
- Mei, Y., Liu, J. & Chen, Z. (2022) Distributionally Robust Second-Order Stochastic Dominance Constrained Optimization with Wasserstein Ball. *SIAM Journal on Optimization*, 32:715-738.
- Miao, Z., Cai, S. & Xu, D. (2014). Applying an adaptative tabu-search algorithm to optimize truck-door assignment in the crossdock management system. *Expert Systems with Applications* 4:16-22.
- Mousavi, S.M., Behnam Vahdani, B., Tavakkoli-Moghaddam, R. & Hashemi, H. (2014). Location of cross-docking centers and vehicle routing scheduling under uncertainty: A fuzzy possibilistic-stochastic programming model. *Applied Mathematical Modeling*, 38:2249-2264.
- Nassief, W. (2017). Cross-dock door assignments: Models, algorithm and extensions. PhD Thesis, Concordia University. Montreal, Canada.
- Nassief, W., Contreras, I. & Jaumard, B. (2018). A comparison of formulations and relaxations for the cross-dock door assignment problems. *Computers & Operations Research*, 94:76-88.
- Nassief, W., Contreras, I., Guignard, M., Hahn, P. & Jaumard, B. (2019). The container scheduling and cross-dock door selection problem. *Journal of the Operational Research Society*, submitted for publication.

- Oliveira, W. de (2021). Risk-Averse Stochastic Programming and Distributionally Robust Optimization Via Operator Splitting. *Set-Valued and Variational Analysis*, 29:861-891.
- Pardo, L (2005) *Statistical inference based on divergence measures*. CRC Press.
- Pflug, G.C. & Pichler, A. (2014). A distance of multi-stage stochastic optimization models. *SIAM Journal on Optimization*, 22:1-22.
- Pichler, A. (2024). Connection between higher order measures of risk and stochastic dominance. *Computational Management Science*, 21:41.
- Philpott, A.B., de Matos, V.L. & Kapelevich, L. (2018). Distributionally robust SDDP. *Computational Management Science*, 15:431-454.
- The R Project for Statistical Computing. Available: www.r-project.org.
- Ross, J. 1997. Office Depot scores major cross-docking gains. *Sore Magazine*, 39.
- Saif, A. & Delage, E. (2021). Data-driven distributionally robust capacity facility location. *European Journal of Operational Research*, 29:995-1007.
- Scarf, H.E. (1957). A min-max solution of an inventory problem. Technical report P-910, Rand Corporation, Santa Monica, CA, USA.
- Serrano, Ch., Delorme, X. & Dolgui A. (2021). Cross-dock distribution and operation planning for overseas delivery consolidation. *CIRP Journal of Manufacturing Science and Technology*, 33:71-81.
- Shapiro, A. (2021). Tutorial on risk neutral, distributionally robust and risk averse multistage stochastic programming. *European Journal of Operational Research*, 288:1-13.
- Shapiro, A., Dentcheva, D. & Ruszczyński, A. (2009). Lectures on Stochastic Programming: Modeling and Theory. *MPS-SIAM Series on Optimization 28*, 3rd edition, <https://doi.org/10.1137/1.9781611976595>.
- Shen H. & Jiang, R. (2023). Chance-constrained set covering with Wasserstein ambiguity. *Mathematical Programming*, 198:621-674.
- Soanpet, A. (2012). Optimization models for locating cross-docks under capacity uncertainty. Graduate Theses, Dissertations, and Problem Reports. 582, West Virginia University, VI, USA. <https://researchrepository.wvu.edu/etd/582>.
- Taheri, F. & Taft, A.F. (2024). Reliable scheduling and routing in robust multiple cross-docking networks design. *Engineering Applications of Artificial Intelligence*, 128:107466.
- Tong, X., Wu, F. & Qi, L. (2009). Worst-case CVaR based portfolio optimization models with application to scenario planning. *Optimization Methods & Software*, 24:933-958.
- VanBelle, J., Valckenaers, P. & Cattrysse, D (2012). Cross-docking: State-of-the-art. *Omega*, 40:827-846.
- Xi, X., Changehun, L., Yuan, W. & Hay, L.L. (2020). Two-stage conflict robust optimization models for cross-dock truck scheduling problem under uncertainty. *Transportation Research E*, 144:102123.
- Xie, W. (2020). Tractable reformulations of two-stage distributionally robust linear programs over the type $-\infty$ Wasserstein ball. *Operations Research Letters*, 48:513-523.
- Wang, D., Yang, K. Yang, L. & Dong, J. (2023). Two-stage distributionally robust optimization for disaster relief logistics under option contract and demand ambiguity. *Transportation Research Part E: Logistics and Transportation Review*, 170:103025.

- Wang, J., Wen, J., Pajic, W. & Andrejic, M. (2024). Optimizing cross-dock terminal location selection: A multi-step approach based on CI-DEA-IDOCRIW-MABAC for enhanced supply chain efficiency - A case study. *Mathematics*, 12, 736.
- Zhai, J., Yu, H., Liang, K.-R., & Li, K.W. (2025). Distributionally robust optimization of a newsvendor model under capital constraint and risk aversion. *Computers & Operations Research*, 106870.
- Zhu, S. & Fukushima, M. (2009). Worst-case conditional value-at-risk with application to robust portfolio management. *Operations Research*, 57:1155-1168.

Two-stage Distributionally Robust Optimization for Cross-dock Door Design. Appendices

A CDDP-TS stochastic elements

For completeness, this appendix provides the additional elements to those that are considered in Section 3.1, see also [Escudero et al. \(2024b\)](#).

Cross-dock infrastructure. Elements

First stage parameters, for $i \in \mathcal{I}$, $j \in \mathcal{J}$

E_{ij} , distance between strip door i and stack door j .

S_{ki} , nominal capacity of alternative level k in strip door i , for $k \in \mathcal{K}_i$.

R_{kj} , nominal capacity of alternative level k in stack door j , for $k \in \mathcal{K}_j$.

F_{ki} , cost of installing capacity level k in strip door i , for $k \in \mathcal{K}_i$.

F_{kj} , cost of installing capacity level k in stack door j , for $k \in \mathcal{K}_j$.

F_0 , high enough penalization for considering outsourcing ‘doors’ $i = 0$ and $j = 0$.

\bar{I} and \bar{J} , upper bounds on the number of strip and stack doors, respectively, that are allowed in the CD infrastructure.

Accepted door set for origin-destination nodes under scenario ω , for $\omega \in \Omega_p$, $p \in \mathcal{P}$

$\mathcal{I}_m^\omega \subseteq \mathcal{I}$, subset $\{i\}$ of strip doors to be expressed as

$$\{i \in \mathcal{I} : \exists k \in \mathcal{K}_i \text{ where } S_m^\omega \leq (1 - D_i^\omega)S_{ki}\}, \text{ for } m \in \mathcal{M}^\omega.$$

$\mathcal{J}_n^\omega \subseteq \mathcal{J}$, subset $\{j\}$ of stack doors to be expressed as

$$\{j \in \mathcal{J} : \exists k \in \mathcal{K}_j \text{ where } R_n^\omega \leq (1 - D_j^\omega)R_{kj}\}, \text{ for } n \in \mathcal{N}^\omega.$$

Second stage parameters for origin node m and destination node n under scenario ω , for $m \in \mathcal{M}^\omega$, $n \in \mathcal{N}^\omega$, $\omega \in \Omega_p$, $p \in \mathcal{P}$

$S_m^\omega = \sum_{n \in \mathcal{N}^\omega} H_{mn}^\omega$, inbound volume to entering through any strip door from m .

$R_n^\omega = \sum_{m \in \mathcal{M}^\omega} H_{mn}^\omega$, outbound volume to exiting through any stack door to node n .

G_{minj}^ω , standard handling and transportation cost of commodity volume H_{mn}^ω , due to entering in the CD from node m through strip door i and exiting to node n through stack door j , based on $E_{ij}H_{mn}^\omega$, for $i \in \mathcal{I}_m^\omega$, $j \in \mathcal{J}_n^\omega$.

G_{minj}^ω for $i = 0$, $j = 0$, high enough penalization for considering the "outsourcing doors".

Second stage binary variables for $m \in \mathcal{M}^\omega$, $n \in \mathcal{N}^\omega$, $\omega \in \Omega$:

$x_{mi}^\omega = 1$, if origin node m is assigned to strip door i ; otherwise, 0, for $i \in \mathcal{I}_m^\omega$.

$x_{m0}^\omega = 1$, if node m is *not* assigned to any strip door; otherwise, 0.

$y_{nj}^\omega = 1$, if destination node n is assigned to stack door j ; otherwise, 0, for $j \in \mathcal{J}_n^\omega$.

$y_{n0}^\omega = 1$, if node n is *not* assigned to any stack door; otherwise, 0.

The additional constraints referred to in system (4) can be expressed

$$\begin{aligned} x_{mi}^\omega \in \{0, 1\} \quad \forall i \in \mathcal{I}_m^\omega \cup \{0\}, \quad \alpha_0^\omega \in \{0, 1\}, \quad x_{m0}^\omega \leq \alpha_0^\omega, \quad \sum_{i \in \mathcal{I}_m^\omega \cup \{0\}} x_{mi}^\omega = 1 \\ \forall m \in \mathcal{M}^\omega, \omega \in \Omega \end{aligned} \quad (19)$$

$$\sum_{m \in \mathcal{M}^\omega: i \in \mathcal{I}_m^\omega} S_m^\omega x_{mi}^\omega \leq (1 - D_i^\omega) \sum_{k \in \mathcal{K}_i} S_{ki} \alpha_{ki} \quad \forall i \in \mathcal{I}, \omega \in \Omega \quad (20)$$

$$\begin{aligned} y_{nj}^\omega \in \{0, 1\} \quad \forall j \in \mathcal{J}_n^\omega \cup \{0\}, \quad \beta_0^\omega \in \{0, 1\}, \quad y_{n0}^\omega \leq \beta_0^\omega, \quad \sum_{j \in \mathcal{J}_n^\omega \cup \{0\}} y_{nj}^\omega = 1 \\ \forall n \in \mathcal{N}^\omega, \omega \in \Omega \end{aligned} \quad (21)$$

$$\sum_{n \in \mathcal{N}^\omega: j \in \mathcal{J}_n^\omega} R_n^\omega y_{nj}^\omega \leq (1 - D_j^\omega) \sum_{k \in \mathcal{K}_j} R_{kj} \beta_{kj} \quad \forall j \in \mathcal{J}, \omega \in \Omega. \quad (22)$$

The second stage constraint system (19)-(22) defines the assignment and outsourcing constraining in the CD entity under the scenarios. Constraints (19) and (21) force the inbound and outbound outsourcing be activated in case that some assignment of origin nodes to strip doors and destination nodes to stack doors is not possible for a given scenario, respectively. Constraints (20) and (22) upper bound the commodity volume handling in the strip and stack doors, based on the doors' net capacity. On the other hand, the binary quadratic term $x_{mi}^\omega y_{nj}^\omega$ is mathematically equivalent to the replacement with fractional 0-1 variable v_{minj}^ω plus constraint system (23).

$$\begin{aligned} \sum_{j \in \mathcal{J}_n^\omega \cup \{0\}} v_{minj}^\omega &= x_{mi}^\omega \quad \forall i \in \mathcal{I}_m^\omega \cup \{0\}, m \in \mathcal{M}^\omega, n \in \mathcal{N}^\omega, \omega \in \Omega \\ \sum_{i \in \mathcal{I}_m^\omega \cup \{0\}} v_{minj}^\omega &= y_{nj}^\omega \quad \forall m \in \mathcal{M}^\omega, j \in \mathcal{J}_n^\omega \cup \{0\}, n \in \mathcal{N}^\omega, \omega \in \Omega \\ v_{minj}^\omega &\geq 0 \quad \forall i \in \mathcal{I}_m^\omega \cup \{0\}, m \in \mathcal{M}^\omega, j \in \mathcal{J}_n^\omega \cup \{0\}, n \in \mathcal{N}^\omega, \omega \in \Omega. \end{aligned} \quad (23)$$

And, the term introduced in the definition of \hat{F}^ω (4d) is computed as:

$$F(v_{minj}^\omega) = \sum_{m \in \mathcal{M}^\omega} \sum_{i \in \mathcal{I}_m^\omega \cup \{0\}} \sum_{n \in \mathcal{N}^\omega} \sum_{j \in \mathcal{J}_n^\omega \cup \{0\}} G_{minj}^\omega v_{minj}^\omega \quad \forall \omega \in \Omega_p, p \in \mathcal{P}. \quad (24)$$

B Lagrangean Decomposition (LD) of LIP-RN model (3) and LIP-SD model (13)

B.1 LD of LIP-RN (3)

Constraints SVC-RN (5) are to be dualized, so, let us consider the following Lagrange multipliers (LM) $\lambda_{ki}^c \geq 0$ for α -SVC (5a), $\mu_{kj}^c \geq 0$ for β -SVC (5b), and $\phi^c \geq 0$ for u -SVC (5c).

LD of LIP-RN (3) can be expressed, for LM vector $\nu = (\lambda, \mu, \phi)$,

$$z_{LD-RN}(\nu) = \min u^c \quad (25a)$$

$$+ \sum_{c \in \mathcal{C}} \left[\sum_{i \in \mathcal{I}} \sum_{k \in \mathcal{K}_i} \lambda_{ki}^c (\alpha_{ki}^c - \alpha_{ki}^{n(c)}) + \sum_{j \in \mathcal{J}} \sum_{k \in \mathcal{K}_j} \mu_{kj}^c (\beta_{kj}^c - \beta_{kj}^{n(c)}) \right] \quad (25b)$$

$$+ \sum_{c \in \mathcal{C}} \phi^c (u^c - u^{n(c)}) \quad (25c)$$

$$\text{s.to cons system (6b) -- (6d).} \quad (25d)$$

It is well known that a LD solution value is not higher than z_{RN}^* for nonnegative LM elements, see the seminal works [Geoffrion \(1974\)](#), [Guignard and Kim \(1987\)](#). So, $z_{LD-RN}(\nu) \leq z_{RN}^*$. The time honored Lagrangean dual problem consists of obtaining the LM vector ν^* , such that $\nu^* = \argmax_{\nu} \{z_{LD-RN}(\nu)\}$. Anyway, a straightforward solving of model LD-RN is neither intended itself. Moreover, it allows to decompose it in scenario cluster c -submodels $\forall c \in \mathcal{C}$ for easing its solving. There is a broad literature on exact and matheuristic methods for this purpose. [Escudero et al. \(2016\)](#) presents an overview and a computational comparison of some methodologies, such as SM (Subgradient Method), VA (Volume Algorithm), LPHA (Lagrangean Progressive Hedging Algorithm), and DCCP (Dynamic Constrained Cutting Plane). See [Bragin \(2024\)](#) for recent advancements.

Model LD-RN can be decomposed in c -submodels (26), for $c \in \mathcal{C}$, to be expressed

$$z_{LD-RN}^c(\nu) = \min (1 + \phi^c - \phi^{a(c)}) u^c \quad (26a)$$

$$+ \sum_{i \in \mathcal{I}} \sum_{k \in \mathcal{K}_i} (\lambda_{ki}^c - \lambda_{ki}^{a(c)}) \alpha_{ki}^c + \sum_{j \in \mathcal{J}} \sum_{k \in \mathcal{K}_j} (\mu_{kj}^c - \mu_{kj}^{a(c)}) \beta_{kj}^c \quad (26b)$$

$$\text{s.to cons system (7b) -- (7c).} \quad (26c)$$

B.2 LD of LIP-SD (13)

For decomposition purposes, let γ_p , u_p , u from (11) be replaced with γ^c , u_c , $u^c \forall c \in \mathcal{C}_p$, $p \in \mathcal{P}$. Let also \tilde{c} denote any scenario cluster in \mathcal{C}_p , $p \in \mathcal{P}$. Additionally, the constraints γ_p -(14b) are to be dualized, and the constraints u_p -(15b)-(15c), S1 (11c) and SD (12c) are to be Lagrangean Relaxed (LR). So, let the related LM $\delta^c \geq 0$, $\pi_{p(c)} \geq 0$ and $\pi'_{p(c)} \geq 0$ for $p(c) \in \mathcal{P}$, where $c \in \mathcal{C}_p$, the non-signed LM σ , and the LM $\varphi_p^b \geq 0$, for $b \in \mathcal{B}$, $p \in \mathcal{P}$, respectively.

Model LD-SD can be expressed, for the LM vector $\nu = (\lambda, \mu, \phi, \delta, \pi, \pi', \sigma, \varphi)$,

$$z_{LD-SD}(\nu) = \min u^{\tilde{c}} \quad (27a)$$

$$+ \sum_{c \in \mathcal{C}} \left[\sum_{i \in \mathcal{I}} \sum_{k \in \mathcal{K}_i} \lambda_{ki}^c (\alpha_{ki}^c - \alpha_{ki}^{n(c)}) + \sum_{j \in \mathcal{J}} \sum_{k \in \mathcal{K}_j} \mu_{kj}^c (\beta_{kj}^c - \beta_{kj}^{n(c)}) \right] \quad (27b)$$

$$+ \sum_{p \in \mathcal{P}} \sum_{c \in \mathcal{C}_p} \phi^c (u^c - u^{n(c)}) \quad (27c)$$

$$+ \sum_{p \in \mathcal{P}} \sum_{c \in \mathcal{C}_p} \delta^c (\gamma^c - \gamma^{n(c)}) \quad (27d)$$

$$+ \sum_{c \in \mathcal{C}} \pi_{p(c)} (\underline{u}(1 - \gamma^c) + u^c - \tilde{w}^c C_1^c - \sum_{\omega \in \Omega^c} w^\omega F^\omega) \quad (27e)$$

$$+ \sum_{c \in \mathcal{C}} \pi'_{p(c)} (\tilde{w}^c C_1^c + \sum_{\omega \in \Omega^c} w^\omega F^\omega - \tilde{u}^c) \quad (27f)$$

$$+ \sigma \left(\sum_{p \in \mathcal{P}} \gamma^{\tilde{c}_p} - 1 \right) \quad (27g)$$

$$+ \sum_{p \in \mathcal{P}} \sum_{b \in \mathcal{B}} \varphi_p^b \left(\sum_{\omega \in \Omega_p} w^\omega s^{\omega, b} - \bar{s}^b \right) \quad (27h)$$

$$\text{s.to cons system (15b) - (15e).} \quad (27i)$$

Notice that $z_{LD-SD}(\nu) \leq z_{SD}^*$. The expressions (27b)-(27d) take the dualization of SVC-SD (14). The expressions (27e), (27f), (27g) and (27h) take the Lagrangean relaxations of (15b)-(15c), S1 (11c) and SD (12c), respectively.

Model LD-SD can be decomposed in c -submodels (28), for $c \in \mathcal{C}$, to be expressed

$$z_{LD-SD}^c(\nu) = \min (1 + \phi^c - \phi^{a(c)} + \pi_{p(c)} - \pi'_{p(c)}) u^c \quad (28a)$$

$$+ \sum_{i \in \mathcal{I}} \sum_{k \in \mathcal{K}_i} (\lambda_{ki}^c - \lambda_{ki}^{a(c)}) \alpha_{ki}^c + \sum_{j \in \mathcal{J}} \sum_{k \in \mathcal{K}_j} (\mu_{kj}^c - \mu_{kj}^{a(c)}) \beta_{kj}^c \quad (28b)$$

$$+ (\delta^c - \delta^{a(c)} - \pi_{p(c)} \underline{u} + \tilde{w}^c \sigma) \gamma^c \quad (28c)$$

$$+ (\pi'_{p(c)} - \pi_{p(c)}) (\tilde{w}^c C_1 + \sum_{\omega \in \Omega^c} w^\omega F^\omega) \quad (28d)$$

$$+ \sum_{b \in \mathcal{B}} \varphi_{p(c)}^b \sum_{\omega \in \Omega^c} w^\omega s^{\omega, b} \quad (28e)$$

$$\text{s.to cons system (16b) - (16c).} \quad (28f)$$

Note: The SCD-based lower bound (17) of the optimal solution value z_{SD}^* is replaced with the expression

$$\underline{z}_{SD}(\nu) = \max \{ z_{LP-SD}, \max_{p \in \mathcal{P}} \{ \sum_{c \in \mathcal{C}_p} \tilde{w}^c z_{LD-SD}^c(\nu) + \pi_p \underline{u} - \sigma - \sum_{b \in \mathcal{B}} \varphi_p^b \bar{s}^b \} \}. \quad (29)$$

C Data for instance I1

Table 1 summarises some statistics of ℓ_p^ρ retrieved from the solution of Wasserstein model (2) for each of the four PD assumptions in set \mathcal{Q} . The statistics are the minimum, first quartile, median, mean, third quartile and the maximum value in the frequency distribution of the proximities.

Table 1: II. Statistics for *proximity* $\ell_p^\rho \forall p \in \mathcal{P}'_q, q \in \mathcal{Q}$

Distribution	<i>Min</i>	<i>1stQu</i>	<i>Median</i>	<i>Mean</i>	<i>3rdQu</i>	<i>Max</i>
Normal	8.855	9.178	9.367	9.407	9.529	10.210
Weibull	11.540	11.830	11.930	11.970	12.050	12.570
Gamma	9.936	10.267	10.411	10.401	10.560	10.775
Lognormal	10.040	10.270	10.420	10.400	10.520	10.870

It can be seen that the perturbations in the Normal PD are the nearest ones to ND. See in Table 1 the statistics of ℓ_p^ρ for the candidates to become the ambiguity set \mathcal{P} based on the set of the 80 proximities in the experiment. The ambiguity set $\mathcal{P} = \mathcal{P}_{10\%}$ corresponds to the first decile $\theta_{10\%} = 9.338$ as the *radius*; it is composed of the eight consecutively numbered perturbations $p \in \{1, 2, \dots, 8\}$, and, in this case, all of them are Normal. Whereas the ambiguity set $\mathcal{P}_{5\%}$ does it for the first 5-centile reduced *radius* $\theta_{5\%} = 9.145$; it is composed of the first four perturbations $p \in \{1, 2, 3, 4\}$, so that $\mathcal{P}_{5\%} \subset \mathcal{P}_{10\%}$.

Notice in Table 2 that the black swan scenarios $\omega = 5$ in all members and, $\omega = 1$ in members $p = 2$ and 3, have the highest costs (mainly, due to outsourcing) and also sharing a very small weight.

 Table 2: II. Weights and optimal solution of model LIP-RN (3) for the CD node-door assigned costs in scenario ω , for $\omega \in \Omega_p, p \in \mathcal{P}_{5\%}$,

$p = 1$		$p = 2$	
$w^1 = 5.841132e - 06$	$\hat{F}^1 = 5388$	$w^1 = 3.909180e - 05$	$\hat{F}^1 = 12401188$
$w^2 = 6.082577e - 07$	$\hat{F}^2 = 5555$	$w^2 = 4.025044e - 02$	$\hat{F}^2 = 5450$
$w^3 = 7.230249e - 01$	$\hat{F}^3 = 5639$	$w^3 = 7.701221e - 01$	$\hat{F}^3 = 5639$
$w^4 = 2.161435e - 01$	$\hat{F}^4 = 6033$	$w^4 = 1.895883e - 01$	$\hat{F}^4 = 6041$
$w^5 = 2.404819e - 12$	$\hat{F}^5 = 14000416$	$w^5 = 9.389944e - 25$	$\hat{F}^5 = 14400000$
$p = 3$		$p = 4$	
$w^1 = 3.796548e - 07$	$\hat{F}^1 = 14600000$	$w^1 = 7.957016e - 06$	$\hat{F}^1 = 5380$
$w^2 = 3.658705e - 02$	$\hat{F}^2 = 5483$	$w^2 = 5.807343e - 02$	$\hat{F}^2 = 5451$
$w^3 = 7.54214e - 01$	$\hat{F}^3 = 5632$	$w^3 = 7.044399e - 01$	$\hat{F}^3 = 5623$
$w^4 = 2.086911e - 01$	$\hat{F}^4 = 6094$	$w^4 = 2.374787e - 01$	$\hat{F}^4 = 6080$
$w^5 = 8.937330e - 19$	$\hat{F}^5 = 14800000$	$w^5 = 6.835344e - 11$	$\hat{F}^5 = 12401053$

For the SD parameters' triplet ($\iota^1 = 7600$, $\bar{s}^1 = 2500$ i.e., about 35% of the u -value, $\bar{s}^1 = 1500$, i.e. about 20% of u), for $|\mathcal{B}| = 1$ and $1 \in \mathcal{B}$, the optimal cost $z^* = 7459.31$ of model LIP-SD (13) for ambiguity set $\mathcal{P}_{5\%}$ is higher than the RN counterpart 7260.56, see Table 3. It is composed of the first stage infrastructure building cost $\hat{C}_1 = 1764$ and the second stage highest expected cost 5695.31 (where the selected ambiguity set member is $p = 4$, since $\gamma_p = 1$). It can be observed that the solution of the black swan scenarios have not any more negative implication (i.e., outsourcing, in this case) in the SD solution at a reasonable cost z_{SD}^* .

Table 3: I1. Weights and optimal solution of model LIP-SD (13) for the CD node-door assigned costs and cost surplus variables in scenario ω , for $\omega \in \Omega_p$, $p \in \mathcal{P}_{5\%}$

$p = 1$			$p = 2$		
$w^1 = 5.841132e - 06$	$\hat{F}^1 = 5638$	$\hat{s}^1 = 0.0$	$w^1 = 3.909180e - 05$	$\hat{F}^1 = 5342$	$\hat{s}^1 = 0.0$
$w^2 = 6.082577e - 07$	$\hat{F}^2 = 5483$	$\hat{s}^2 = 0.0$	$w^2 = 4.025044e - 02$	$\hat{F}^2 = 5450$	$\hat{s}^2 = 0.0$
$w^3 = 7.230249e - 01$	$\hat{F}^3 = 5639$	$\hat{s}^3 = 0.0$	$w^3 = 7.701221e - 01$	$\hat{F}^3 = 5639$	$\hat{s}^3 = 0.0$
$w^4 = 2.161435e - 01$	$\hat{F}^4 = 5920$	$\hat{s}^4 = 0.0$	$w^4 = 1.895883e - 01$	$\hat{F}^4 = 5929$	$\hat{s}^4 = 0.0$
$w^5 = 2.404819e - 12$	$\hat{F}^5 = 6905$	$\hat{s}^5 = 1069$	$w^5 = 6.835344e - 11$	$\hat{F}^5 = 7375$	$\hat{s}^5 = 1539$

$p = 3$			$p = 4$		
$w^1 = 3.786548e - 07$	$\hat{F}^1 = 5558$	$\hat{s}^1 = 0.0$	$w^1 = 7.957016e - 06$	$\hat{F}^1 = 5187$	$\hat{s}^1 = 0.0$
$w^2 = 3.658705e - 02$	$\hat{F}^2 = 5446$	$\hat{s}^2 = 0.0$	$w^2 = 5.807343e - 02$	$\hat{F}^2 = 5519$	$\hat{s}^2 = 0.0$
$w^3 = 7.54214e - 01$	$\hat{F}^3 = 5632$	$\hat{s}^3 = 0.0$	$w^3 = 7.044399e - 01$	$\hat{F}^3 = 5634$	$\hat{s}^3 = 0.0$
$w^4 = 2.086911e - 01$	$\hat{F}^4 = 5927$	$\hat{s}^4 = 0.0$	$w^4 = 2.374787e - 01$	$\hat{F}^4 = 5920$	$\hat{s}^4 = 0.0$
$w^5 = 8.937330e - 19$	$\hat{F}^5 = 7222$	$\hat{s}^5 = 1386$	$w^5 = 6.835344e - 11$	$\hat{F}^5 = 6921$	$\hat{s}^5 = 1085$

D Data for instance I3

Table 4 summarises some statistics of ℓ_p^ρ retrieved from the solution of Wasserstein model (2) for each of the four PD assumptions in set \mathcal{Q} . Although the Normal PD perturbations are still the closest to ND,

Table 4: Instance I3. Statistics for *proximity* $\ell_p^\rho \forall p \in \mathcal{P}'_q, q \in \mathcal{Q}$

Distribution	<i>Min</i>	<i>1stQu</i>	<i>Median</i>	<i>Mean</i>	<i>3rdQu</i>	<i>Max</i>
Normal	9.91	10.67	10.98	11.03	11.17	14.17
Weibull	11.02	12.35	12.50	12.68	13.09	14.11
Gamma	10.42	10.99	11.42	11.45	11.77	12.63
Lognormal	10.60	11.01	11.60	11.55	11.75	13.27

in this case the Lognormal and Gamma PD perturbations also quite close to ND. See in Table 4 the statistics of ℓ_p^ρ for the candidates to become the ambiguity set \mathcal{P} . That set $\mathcal{P} = \mathcal{P}_{7\%}$ corresponds to the first 7-centile $\theta_{7\%} = 10.61$ as the *radius*; it is composed of the six consecutively numbered perturbations $p \in \{1, 2, \dots, 6\}$, of which the first three are Normal, the fourth and the fifth ones are Gamma and the sixth is Lognormal. Whereas the ambiguity set $\mathcal{P}_{3\%}$ does it for the first 3-centile reduced *radius* $\theta_{3\%} = 10.31$; it is composed of the first three perturbations $p \in \{1, 2, 3\}$, so that $\mathcal{P}_{3\%} \subset \mathcal{P}_{7\%}$.

Table 5 shows the weights and the CD node-door assignment cost under the scenarios in ambiguity set $\mathcal{P}_{3\%}$ retrieved from the incumbent solution of model LIP-RN (3) (instance I3-RN-3), provided by Cplex. The cost $z_{RN}^* = 8451.89$ is composed of the first stage infrastructure building cost $C_1 = 2082$ and the second stage expected cost 6369.89 of ambiguity set member $p = 3 : \gamma_p = 1$. It can be observed the very high cost of the black swan scenarios.

For the SD parameters' triplet ($\iota^1 = 9600$, $\bar{s}^1 = 2500$, $\bar{\bar{s}}^1 = 1500$), for $|\mathcal{B}| = 1$ and $1 \in \mathcal{B}$, the incumbent

Table 5: I3. Weights and Cplex incumbent solution of model LIP-RN (3) for the CD node-door assigned costs under scenario ω , for $\omega \in \Omega_p$, $p \in \Omega_p$, $p \in \mathcal{P}_{3\%}$

$p = 1$		$p = 2$	
$w^1 = 3.218249e - 06$	$\hat{F}^1 = 5584$	$w^1 = 1.228770e - 04$	$\hat{F}^1 = 5775$
$w^2 = 3.907031e - 02$	$\hat{F}^2 = 5623$	$w^2 = 4.996638e - 02$	$\hat{F}^2 = 5543$
$w^3 = 2.921724e - 01$	$\hat{F}^3 = 5624$	$w^3 = 3.363456e - 01$	$\hat{F}^3 = 5703$
$w^4 = 1.687540e - 01$	$\hat{F}^4 = 5932$	$w^4 = 1.135651e - 01$	$\hat{F}^4 = 6014$
$w^5 = 1.684348e - 10$	$\hat{F}^5 = 9803406$	$w^5 = 3.508562e - 12$	$\hat{F}^5 = 14200432$
$w^6 = 3.727733e - 08$	$\hat{F}^6 = 9405025$	$w^6 = 2.333095e - 09$	$\hat{F}^6 = 9203768$
$w^7 = 9.015966e - 03$	$\hat{F}^7 = 6940$	$w^7 = 3.080624e - 03$	$\hat{F}^7 = 6888$
$w^8 = 4.071194e - 01$	$\hat{F}^8 = 7111$	$w^8 = 4.551538e - 01$	$\hat{F}^8 = 7159$
$w^9 = 8.386457e - 02$	$\hat{F}^9 = 7703$	$w^9 = 4.176560e - 02$	$\hat{F}^9 = 7685$
$w^{10} = 9.389927e - 21$	$\hat{F}^{10} = 15003648$	$w^{10} = 4.330379e - 18$	$\hat{F}^{10} = 15001678$

$p = 3$	
$w^1 = 1.020567e - 07$	$\hat{F}^1 = 13200432$
$w^2 = 7.065075e - 02$	$\hat{F}^2 = 5501$
$w^3 = 2.021934e - 01$	$\hat{F}^3 = 5592$
$w^4 = 2.271557e - 01$	$\hat{F}^4 = 5948$
$w^5 = 3.077295e - 18$	$\hat{F}^5 = 9801489$
$w^6 = 5.518698e - 11$	$\hat{F}^6 = 18801824$
$w^7 = 1.757278e - 03$	$\hat{F}^7 = 6637$
$w^8 = 4.599281e - 01$	$\hat{F}^8 = 7201$
$w^9 = 3.831462e - 02$	$\hat{F}^9 = 7539$
$w^{10} = 2.904815e - 27$	$\hat{F}^{10} = 15001564$

cost $z_{SD} = 8526.87$ of model LIP-SD (13) is composed of the first stage infrastructure building cost $\hat{C}_1 = 2082$ and the second stage expected cost 6444.87 in ambiguity set member $p = 3 : \gamma_p = 1$, for $p \in \mathcal{P}_{3\%}$. The total cost $\hat{C}_{12,p=3}^\omega$, see Section 4.1, is composed of \hat{C}_1 plus the second stage cost \hat{F}^ω for scenario ω . Table 6 shows some results retrieved from the incumbent solution of models LIP-RN (3) and LIP-SD (13), as the cost \hat{F}^ω of the CD node-door assignment, the total cost $\hat{C}_{12,p=3}^\omega$ and the values of the surplus cost variables $s^{\omega,1}$. It can be seen that the s -variables in the incumbent RN solution have zero-values for all scenarios in the SD version, but for scenario $\omega = 10$, which value is smaller than bound \bar{s}^1 in SD constraint (12b). On the other hand, this value is not high enough to violate the bound \bar{s}^1 for the expected surplus cost in SD constraint (12c).

Table 7 shows the matheuristic incumbent solution of models LIP-RN (3) and LIP-SD (13), see Sections 3.4 and 4.3 in ambiguity set $\mathcal{P}_{3\%}$. The solution ($\bar{z}_H = 8320.96, \hat{C}_1 = 1849$) for I3-RN-3 violates the non-imposed upper bound $\bar{s}^1 = 2500$ in the black swan scenarios. The solution $\bar{z}_H = 8503.66, \hat{C}_1 = 2082$ for I3-SD-3 does not violate the SD constraints.

In a similar way to $\mathcal{P}_{3\%}$, Table 8 shows the matheuristic incumbent solution of models LIP-RN (3) and LIP-SD (13) in ambiguity set $\mathcal{P}_{7\%}$. The solution ($\bar{z}_H = 8327.80, \hat{C}_1 = 1849$) for I3-RN-6 violates

Table 6: I3. Cplex incumbent solution of models LIP-RN (3) and LIP-SD (13), in particular surplus cost variables for the selected member $p = 3$: $\gamma_3 = 1$ in ambiguity set $\mathcal{P}_{3\%}$

	I3-RN-3			I3-SD-3		
	\hat{F}^ω	$C_{12,p=3}^\omega$	$\hat{s}^{\omega,1}$	\hat{F}^ω	$C_{12,p=3}^\omega$	$\hat{s}^{\omega,1}$
$w^1 = 1.020567e - 07$	13200432	13202514	13192914	5603	7685	0
$w^2 = 7.065075e - 02$	5501	7583	0	5466	7548	0
$w^3 = 2.021934e - 01$	5592	7674	0	5602	7684	0
$w^4 = 2.271557e - 01$	5948	8030	0	5910	7992	0
$w^5 = 3.077295e - 18$	9801489	9803571	9793971	7480	9562	0
$w^6 = 5.518698e - 11$	18801824	18803906	18794306	6673	8755	0
$w^7 = 1.757278e - 03$	6637	8719	0	6658	8740	0
$w^8 = 4.599281e - 01$	7201	9283	0	7142	9224	0
$w^9 = 3.831462e - 02$	7539	9621	21	7491	9573	0
$w^{10} = 2.904815e - 27$	15001564	1553646	14994046	9405	11487	1887

Table 7: I3. Matheuristic incumbent solution of models LIP-RN (3) and LIP-SD (13), in particular, the surplus cost variables for the selected member $p = 3$: $\gamma_3 = 1$ in ambiguity set $\mathcal{P}_{3\%}$

	I3-RN-3			I3-SD-3		
	\hat{F}_H^ω	$\hat{C}_{12,p=3}^\omega$	$\hat{s}^{\omega,1}$	\hat{F}_H^ω	$\hat{C}_{12,p=3}^\omega$	$\hat{s}^{\omega,1}$
$w^1 = 1.020567e - 07$	14800000	14801849	14792276	5640	7722	0
$w^2 = 7.065075e - 02$	5490	7339	0	5466	7548	0
$w^3 = 2.021934e - 01$	5617	7466	0	5592	7674	0
$w^4 = 2.271557e - 01$	5998	7847	0	5910	7792	0
$w^5 = 3.077295e - 18$	14800000	14801849	14792276	7601	9683	110
$w^6 = 5.518698e - 11$	22000000	22001849	21992276	7027	9109	0
$w^7 = 1.757278e - 03$	6738	8587	0	6648	8730	0
$w^8 = 4.599281e - 01$	7159	9008	0	7099	9181	0
$w^9 = 3.831462e - 02$	7549	9398	0	7459	9541	0
$w^{10} = 2.904815e - 27$	22000000	22001849	21992276	9344	11426	1853

the non-imposed upper bound $\bar{s}^1 = 2500$. The solution ($\bar{z}_H = 8503.94$, $\hat{C}_1 = 2089$) for I3-SD-3 does not violate the SD constraints.

E Data for instance I7

Table 9 summarises some statistics of ℓ_p^ρ retrieved from the solution of Wasserstein model (2) for each of the four PD assumptions in set \mathcal{Q} .

As can be seen, in this case the Gamma and Lognormal PD perturbations are the closest to ND. See in Table 7 the statistics of ℓ_p^ρ for the candidates to become the ambiguity set \mathcal{P} . That set $\mathcal{P} = \mathcal{P}_{7\%}$ corresponds to the first 7-centile $\theta_{7\%} = 12.58$ as the *radius*; it is composed of the six consecutively numbered perturbations $p \in \{1, 2, \dots, 6\}$, of which the second and the third ones are Lognormal, the sixth is Weibull and, the rest are Gamma. Whereas the ambiguity set $\mathcal{P}_{3\%}$ does it for the first 3-centile reduced *radius* $\theta_{3\%} = 12.29$; it is composed of the first three perturbations $p \in \{1, 2, 3\}$, so that $\mathcal{P}_{3\%} \subset \mathcal{P}_{7\%}$, of

Table 8: I3. Matheuristic incumbent solution of models LIP-RN (3) and LIP-SD (13), in particular, the surplus cost variables for the selected member $p = 3$: $\gamma_3 = 1$ in ambiguity set $\mathcal{P}_{7\%}$

	I3-RN-6			I3-SD-6		
	\hat{F}_H^ω	$\hat{C}_{12,p=3}^\omega$	$\hat{s}^{\omega,1}$	\hat{F}_H^ω	$\hat{C}_{12,p=3}^\omega$	$\hat{s}^{\omega,1}$
$w^1 = 1.020567e - 07$	14800000	14801849	14792276	5334	7623	0
$w^2 = 7.065075e - 02$	5503	7532	0	5466	7555	0
$w^3 = 2.021934e - 01$	5634	7483	0	5592	7681	0
$w^4 = 2.271557e - 01$	5998	7844	0	5910	7999	0
$w^5 = 3.077295e - 18$	14800000	14801849	14792276	7629	9718	170
$w^6 = 5.518698e - 11$	22000000	22001849	21992276	6822	8911	0
$w^7 = 1.757278e - 03$	6689	8538	0	6710	8799	0
$w^8 = 4.599281e - 01$	7159	9008	0	7099	9188	0
$w^9 = 3.831462e - 02$	7595	9444	0	7459	9548	0
$w^{10} = 2.904815e - 27$	22000000	22001849	21992276	9224	11313	1765

Table 9: I7. Statistics for *proximity* $\ell_p^p \forall p \in \mathcal{P}'_q, q \in \mathcal{Q}$

Distribution	<i>Min</i>	<i>1stQu</i>	<i>Median</i>	<i>Mean</i>	<i>3rdQu</i>	<i>Max</i>
Normal	13.87	14.16	14.70	14.98	15.12	17.53
Weibull	12.53	13.52	13.71	13.87	14.12	15.88
Gamma	11.80	12.80	13.34	13.40	14.01	14.88
Lognormal	12.19	13.20	13.55	13.48	13.80	14.41

which the first one is one Gamma and and the other two Lognormal.

For the SD parameters' triplet ($\iota^1 = 38800$, $\bar{s}^1 = 7900$, $\bar{\bar{s}}^1 = 7900$), for $|\mathcal{B}| = 1$ and $1 \in \mathcal{B}$, Table 10 shows the matheuristic incumbent solution of models LIP-RN-3 (3) and LIP-SD-3 (13) in ambiguity set $\mathcal{P}_{3\%}$.

The RN solution provided by the proposed matheuristic, see Sections 3.4 and 4.3, ($\bar{z}_H = 22402.18$, $\hat{C}_1 = 7157$) for I7-RN-3 in member $p = 3$ does not satisfy the non-imposed upper bound $\bar{s}^1 = 7900$ in ambiguity set $\mathcal{P}_{3\%}$. However, the matheuristic SD solution ($\bar{z}_H = 22402.69$, $\hat{C}_1 = 7284$) for I7-SD-3 in member $p = 1$ satisfies the SD constraints and, then, it can be observed that the black swan scenarios have not, any more, so negative implications in the SD-solution with a minimal increase of the z -cost.

For the same SD parameter triplet, Table 11 shows the matheuristic incumbent solutions of models LIP-RN-6 (3) and LIP-SD-6 (13), in particular, the surplus cost variables for the selected member $p = 6$: $\gamma_p = 1$ in ambiguity set $\mathcal{P}_{7\%}$, for the instances I7-RN-6 ($\bar{z}_H = 23700.67$, $\hat{C}_1 = 7784$) and I7-SD-6 ($\bar{z}_H = 23939.31$, $\hat{C}_1 = 8023$). It can be observed that the black swan scenarios in model LIP-RN (3) have not, any more, so negative implications in the SD-solution with a minimal increase in z -cost and, additionally, the SD bounds $\bar{s}^1 = 7900$ and $\bar{\bar{s}}^1 = 7000$ are satisfied.

Table 10: I7. Matheuristic incumbent solution of models LIP-RN-3 (3) and LIP-SD-3 (13), in particular, the surplus cost variables for the selected members $p = 3 : \gamma_3 = 1$ (RN) and $p = 1 : \gamma_1 = 1$ (SD) for ambiguity set $\mathcal{P}_{3\%}$

I7-RN-3				I7-SD-3			
weight for $p = 3$	\hat{F}_H^ω	$\hat{C}_{12,p=3}^\omega$	$\hat{s}^{\omega,1}$	weights $p = 1$	\hat{F}_H^ω	$\hat{C}_{12,p=1}^\omega$	$\hat{s}^{\omega,1}$
$w^1 = 5.890609e - 05$	5026	12183	0	5.034938e-05	5120	12404	0
$w^2 = 1.113443e - 01$	5372	12527	0	1.522775e-01	5237	12521	0
$w^3 = 1.140110e - 01$	5519	12676	0	6.236860e-02	5663	12947	0
$w^4 = 2.458577e - 02$	5791	12948	0	3.530357e-02	5819	13103	0
$w^5 = 1.597404e - 12$	6505	13662	0	9.910015e-13	6496	13780	0
$w^6 = 2.151672e - 13$	5808	12965	0	1.085449e-11	5905	13189	0
$w^7 = 3.399928e - 02$	6425	13582	0	1.473375e-02	6323	13607	0
$w^8 = 2.156317e - 01$	6612	13769	0	2.348509e-01	6628	13912	0
$w^9 = 3.690257e - 04$	7028	14185	0	4.153145e-04	6848	14132	0
$w^{10} = 1.182285e - 18$	7727	14884	0	1.341637e-28	8259	15543	0
$w^{11} = 1.717728e - 17$	14252	21409	0	2.357762e-16	14220	21504	0
$w^{12} = 1.142020e - 03$	14945	22102	0	5.588144e-04	15053	22337	0
$w^{13} = 2.488110e - 01$	16000	23157	0	2.492375e-01	15863	23147	0
$w^{14} = 4.698466e - 05$	16910	24067	0	2.036854e-04	16706	23990	0
$w^{15} = 1.111944e - 47$	18697	25854	0	1.124869e-51	18818	26102	0
$w^{16} = 1.445404e - 36$	29396	36553	0	5.365765e-38	29135	36419	0
$w^{17} = 2.012968e - 09$	31040	38197	0	1.650646e-09	30573	37857	0
$w^{18} = 2.500000e - 01$	32918	40705	1275	2.500000e-01	32557	39861	1061
$w^{19} = 3.104054e - 08$	22000000	22007157	21968357	1.794206e-09	34757	42041	3241
$w^{20} = 7.772709e - 97$	22000000	22007157	21968357	1.737634e-72	39408	46692	7892

References

- Bragin, M.A. (2024). Survey on Lagrangian relaxation for MILP: importance, challenges, historical review, recent advancements, and opportunities. *Annals of Operations Research*, 333, 29–45.
- Escudero, L.F., Garín, A. & Unzueta, A. (2016). Cluster Lagrangean decomposition in multistage stochastic optimization *Computers and Operations Research*, 67:48-62.
- Escudero, L.F., Garín, M.A. & Unzueta, A. (2024b). A methodology for the cross-dock door platforms design under uncertainty. *arXiv:arXiv:2403.03686*.
- Geoffrion, A.M. 1974. Lagrangean relaxation for integer programming. *Mathematical Programming Studies*, 2:82-114.
- Guignard, M. & Kim, S. (1987). Lagrangean decomposition. A model yielding stronger Lagrangean bounds. *Mathematical Programming*, 39:215-228.

Table 11: I7. Matheuristic incumbent solutions of models LIP-RN-6 (3) and LIP-SD-6 (13), in particular, the surplus cost variables for the selected member $p = 6$: $\gamma_6 = 1$ in ambiguity set $\mathcal{P}_{7\%}$

	I7-RN-6			I7-SD-6		
weight for $p = 6$	\hat{F}_H^ω	$\hat{C}_{12,p=3}^\omega$	$\hat{s}^{\omega,1}$	\hat{F}_H^ω	$\hat{C}_{12,p=1}^\omega$	$\hat{s}^{\omega,1}$
$w^1 = 6.231762e - 05$	5185	12969	0	5185	13208	0
$w^2 = 5.578641e - 02$	5350	13134	0	5350	13373	0
$w^3 = 1.190980e - 01$	5551	13335	0	5551	13574	0
$w^4 = 7.505325e - 02$	5827	13611	0	5839	13862	0
$w^5 = 1.286116e - 15$	6703	14487	0	6703	14726	0
$w^6 = 2.679631e - 08$	5954	13738	0	5954	13977	0
$w^7 = 1.521364e - 03$	6336	14120	0	6336	14359	0
$w^8 = 4.956362e - 02$	6545	14329	0	6545	14568	0
$w^9 = 1.989150e - 01$	7015	14799	0	7015	15038	0
$w^{10} = 1.380043e - 31$	7774	15558	0	7811	15834	0
$w^{11} = 8.606838e - 18$	14295	22079	0	14298	22321	0
$w^{12} = 1.413645e - 07$	15190	22974	0	15194	23217	0
$w^{13} = 1.715785e - 03$	15914	23698	0	15900	23923	0
$w^{14} = 2.482841e - 01$	16608	24392	0	16597	24620	0
$w^{15} = 3.971946e - 47$	18831	26615	0	18889	26912	0
$w^{16} = 1.731425e - 38$	29447	37231	0	29289	37312	0
$w^{17} = 1.524912e - 16$	31342	39126	326	31142	39165	365
$w^{18} = 1.520760e - 05$	33018	40802	2002	32632	40655	1855
$w^{19} = 2.499848e - 01$	34557	42341	3541	34567	42590	3790
$w^{20} = 8.559141e - 75$	22000000	22007784	21968984	38521	46544	7744